

Geometrically Graded h - p Quadrature Applied to the Complex Boundary Integral Equation Method for the Dirichlet Problem with Corner Singularities

David De Wit

November 1992

Abstract

Boundary integral methods for the solution of boundary value PDEs are an alternative to ‘interior’ methods, such as finite difference and finite element methods. They are attractive on domains with corners, particularly when the solution has singularities at these corners. In these cases, interior methods can become excessively expensive, as they require a finely discretised 2D mesh in the vicinity of corners, whilst boundary integral methods typically require a mesh discretised in only one dimension, that of arc length.

Consider the Dirichlet problem. Traditional boundary integral methods applied to problems with corner singularities involve a (real) boundary integral equation with a kernel containing a logarithmic singularity. This is both tedious to code and computationally inefficient. The CBIEM is different in that it involves a complex boundary integral equation with a smooth kernel. The boundary integral equation is approximated using a collocation technique, and the interior solution is then approximated using a discretisation of Cauchy’s integral formula, combined with singularity subtraction.

A high order quadrature rule is required for the solution of the integral equation. Typical corner singularities are of square root type, and a ‘geometrically graded h - p ’ composite quadrature rule is used. This yields efficient, high order solution of the integral equation, and thence the Dirichlet problem.

Implementation and experimental results in MATLAB code are presented.

1 Introduction

This report describes a research project carried out from March to October 1992, at the Department of Mathematics, The University of Queensland, Australia. It was carried out under the supervision of Dr Graeme A. Chandler, and was accredited as a #30 project, coded MN882.

Techniques related to the CBIEM have been analysed in [20], and used in [9, 8]. The CBIEM is also closely related to the ‘Complex Variable Boundary Element Method’ [15]. This report contains an application of it, using h - p quadrature to achieve high rates of convergence, even in the presence of corner singularities. This application owes its conception to my supervisor.

The ideas of graded meshes and h - p quadrature (numerical integration) are presented in §2, and are illustrated by experimental results. The CBIEM itself is described in §3. §4 details numerical implementation of the CBIEM, using the quadrature technique described in §2, and presents error results for some test problems. §5 concludes the report with suggestions for further development. MATLAB code written for the implementation is listed in Appendix A.

2 h - p Quadrature Methods

2.1 Introduction

This section describes a high order numerical integration (quadrature) technique, that retains its high order in the case of end point singularities in the integrand. The method uses a *graded mesh*, with integration rules of high order used on larger intervals, and low order on smaller intervals. To achieve the ‘best’ possible convergence rates, whilst including the end points of each interval, the basic quadrature rules used are Gauß–Lobatto. The underlying mesh is graded in a *geometric* manner. As the method of using different quadrature rules on internal intervals is a generalisation of earlier ‘ h ’ and ‘ p ’ methods, the resulting composite quadrature rule is called a ‘geometrically graded h - p ’ method [1].

2.2 Quadrature Methods – the Questions

Given an integrand $f : [a, b] \mapsto \mathbb{R}$, consider the numerical approximation of the definite integral by a rule $\{x_k, w_k\}$ on n points:

$$\int_a^b f(x) dx \approx \sum_{k=1}^n f(x_k) w_k.$$

The interval $[a, b]$ is possibly infinite or semi-infinite, but this report considers only finite intervals; and without loss of generality, let $[a, b] = [0, 1]$. Similarly, the integrand could include a weighting factor $\omega(x)$, but this is not required here.

The *degree* of a quadrature rule is the maximal degree of the polynomial that it can integrate exactly.¹ That is, if the degree of a rule on n points is p , then:

$$\int_0^1 x^j dx = \sum_{k=1}^n x_k^j w_k, \quad j = 0 : p.$$

If f is smooth, the rate of convergence for n point Gaußian quadrature is $\mathcal{O}(\rho^n)$ (for some $\rho < 1$), and for the composite Simpson’s rule it is $\mathcal{O}(n^{-4})$. That is, the error decreases more quickly for Gaußian quadrature. This is *not* true in general if f has a singularity.² For example, consider the ‘square root’ singularity $f(x) = \sqrt{x}$, $x \in [0, 1]$. In this case, the rate of convergence for Gaußian quadrature falls to $\mathcal{O}(n^{-3})$, whilst that of Simpson’s rule is $\mathcal{O}(n^{-3/2})$. Even so, using a *composite* Simpson’s rule and a *graded mesh*, a convergence rate of $\mathcal{O}(n^{-4})$ can be recovered.

A *composite* quadrature rule is created by subdividing the interval of integration into m subintervals, and evaluating the integral over each subinterval using an appropriate quadrature rule. Choosing $x_{j-1} < x_j$, $j = 1 : m$, and $x_0 = 0$, $x_m = 1$:

$$\int_0^1 f(x) dx = \sum_{j=1}^m \int_{x_{j-1}}^{x_j} f(x) dx.$$

¹Comments on errors refer to discretisation, not machine roundoff error unless explicitly stated.

²‘Singularity’ is intended to always mean ‘end point singularity’. If a particular singularity in the integrand is not at an end point, then the interval can be subdivided so that the singularity is at the end points of the two subintervals. Most quadrature methods perform poorly on integrands with internal singularities.

Grading the mesh means that the subdivision is organised in some way. A description of a generalised mesh grading to cater for complicated possibilities, such as *adaptive* quadrature is found in [5]. Here, the simplification of nonadaptive meshes is used. Meshes are graded by assigning mesh points according to some simple function. A quadrature rule of degree p_j (a function of n_j , the number of points used by the rule) is used on the interval $[x_{j-1}, x_j]$. This raises two issues:

- How should x_j and n_j be chosen? That is, how should the mesh be graded, and how should the degree of the quadrature rules on each subinterval vary?
- How is this procedure dependent on the integrand? Consider the generalisation of \sqrt{x} to $|x|^\alpha$, or more pathological cases. For experimental work, a known integrand is easy to deal with. What of more general cases, where no explicit functional information is known?

The remainder of this section describes some partial answers to these questions, and displays some experiments. The answers deal with the case $|x|^\alpha$, $-1 < \alpha < 1$, and the experiments demonstrate the case $\alpha = 1/2$.

2.3 Gaußian Quadrature

Gaußian quadrature rules are the *best* possible rules in the sense that they are of maximal degree.³ This is due to the exploitation of the maximal number of degrees of freedom in the choice of their nodes and weights. Gauß methods divide into categories depending on the associated weight function, and whether there are any prescribed quadrature points. For the applications in this report, it is preferable to use the end points of the interval as quadrature points, and a unit weight function is assumed. The appropriate set of rules are called the Gauß–Lobatto rules [6, pages 101–104].

Theorem 2.1 (Gauß–Lobatto Quadrature)

Given $f \in C^{2n-2} [a, b]$, the n point Gauß–Lobatto quadrature rule ($n \geq 2$), has nodes $a \equiv x_1 < x_2 < \dots < x_{n-1} < x_n \equiv b$, and positive weights w_1, \dots, w_n such that:

$$\int_a^b f(x) dx = \sum_{k=1}^n f(x_k) w_k + E_n.$$

Here E_n is dependent on f , a , b and n :

$$E_n = -\frac{n(n+1)[(n-2)!]^4}{(2n-1)[(2n-2)!]^3} (b-a)^{2n-1} f^{(2n-2)}(\xi), \quad \xi \in (a, b). \quad (1)$$

The rule is of degree $p = 2n - 3$ (this is always odd). Observe that for $n = 2$ the rule is the trapezoidal rule, and for $n = 3$ it is Simpson’s rule. Only for $n \geq 4$ do these rules diverge from the series of closed Newton–Cotes rules (see Table 1 on page 8).

An algorithm [11] for finding $\{x_k, w_k\}$ using a matrix eigenvalue technique is implemented in Appendix A.9.

³This may of course, not be ideal for the particular application, but in the absence of theoretical functional information about the integrand, nothing beyond this can be said about the convergence rates of *any* quadrature method. In practice, with commonly occurring functions, there is a certain amount of implicit theoretical information which can be used in error analysis.

2.4 Graded Meshes

A number of different methods for grading meshes appear in the literature. Three important methods [19] are described below. In each case, the mesh subdivides the interval $[0, 1]$, when the integrand has a singularity at 0. The meshes have m subintervals, that is $m + 1$ points, including the ends. The j th mesh point is at x_j , and the j th interval is of width h_j :

1. *Quasiuniform.* The mesh is essentially uniform; that is for some constant $\tau < 1$, $h_j \in [h\tau, h]$, $j = 1 : m - 1$, where $h = \max_j \{h_j\}$.
2. *Algebraic.* For some $\gamma \geq 1$, $x_j = \left(\frac{j}{m}\right)^\gamma$, $j = 0 : m$.
3. *Geometric.* For some $0 < \sigma < 1$, $x_j = \sigma^{m-j}$, $j = 1 : m$; and $x_0 = 0$.

A geometrically graded mesh is illustrated on one segment of a closed contour in Figure 4 on page 19.

2.5 h , p and h - p Quadrature Methods

The ‘ h - p ’ nomenclature presented here originated in papers by Babuška et al. [1, 12, 13, 14], on finite element methods, based on previous work which did not explicitly use this schema. The following discussion of the three methods refers to their use with *graded* meshes.

2.5.1 h Methods

An h quadrature method is composed using two steps:

1. Choose an underlying mesh of subintervals; possibly a graded mesh determined by the user, from analysis of the singularities of the integrand.
2. Integrate over each of the m mesh intervals, applying the same n point quadrature rule. The result is a composite quadrature rule on a total of N points. These N points will be called the *node* points from now on. The functional relationship $N(m, n)$ is dependent on whether the basic quadrature rule is open or closed. (If the rule is open, the original mesh points are not included in the final rule.) Observe that the user cannot arbitrarily select N , only m and n .

$$N(m, n) = \begin{cases} m(n-2) + m + 1 & \text{(closed basic rule)} \\ mn & \text{(open basic rule).} \end{cases}$$

A particular basic rule is decided upon (e.g. Simpson’s rule), and desired accuracy is hopefully attained by simply increasing m (that is, N). Whatever grading is chosen, the separation of the node points (h) decreases as m is increased, hence the name ‘ h method’. For a uniform mesh (which works well for smooth integrands), $h = (b - a) / (N - 1)$ is constant. Alternatively, open rules, or Gauß rules can be used, the only important factor is that all the basic rules are of the same type and degree.

2.5.2 p Methods

In a p method, again a graded mesh is created. Integration is performed over each mesh interval using a basic quadrature rule on n points. Here, n instead of m is varied by the user. That is, for a given number of mesh subintervals, m , a set of rules of increasing degree (that is n , the number of points involved) is used, until desired accuracy is obtained. The same functional relationship $N(m, n)$ exists. As n is increased, the rules used grow in their degree (p), hence the name ‘ p method’ (see also Table 1).

To illustrate, consider the family of closed Newton–Cotes rules. Assume that the interval has been subdivided, possibly using an adaptive algorithm that chooses smaller subdivisions where there the integrand has greater derivative. Approximate the integral over each division using the trapezoidal rule ($p = 1$), and inspect the result. If it is unacceptable, repeat using Simpson’s rule ($p = 3$). Continue this process until results are acceptable.

2.5.3 h - p Methods

The h - p method is the natural combination of the two previous methods. The user may vary both m and n . The idea behind this is to create a composite rule that minimises errors in the approximation, for a given number of node points N . (Experiment demonstrates that this is achievable.) The user chooses a family of basic quadrature rules, then decides how to vary n with mesh interval. As the singularities considered are *always* at end points, a good choice is to organise small mesh intervals and low degree rules (small n) near the end points, and larger mesh intervals and high degree rules away from them, where the integrand is expected to be smooth.

A simple choice is to begin with a rule on $n = 2$ points on the smallest interval, then linearly increase n with the number of the mesh interval. Other discrete integer functions n_j , $j = 1 : m$ are easily designed. The only constraint on these functions is that if any error analysis is to be done, there should be some regularity in n_j . (Choosing basic rules from the same family facilitates this.) This implementation uses the Gauß–Lobatto rule of degree 1 ($n = 2$) on the first interval, degree 3 ($n = 3$) on the second, etc.

Creating the composite quadrature rule is quite difficult. Each of the basic quadrature rules must be appropriately scaled and shifted, and then coincident mesh points must be combined. This is further complicated in the cases of closed meshes, closed quadrature rules, and contour integration, where the end points of various segments of the parameterisation must also be combined. (This is exacerbated if the contour is closed.) The CBIEM requires all of these to be implemented. The (closed) contours involved have corners, and the integrand will usually have singularities at these corners. As it will be important to keep the collocation points (see §3.2.3) between, and not on, the corners, the underlying meshes *must* include end points. This means that the basic quadrature rules must be closed, so as to include the end points.

The literature recommends using a geometrically graded mesh, with an h - p quadrature method. (This is implemented in the CBIEM.) For maximum efficacy, the basic quadrature rules chosen must be of maximal degree, which restricts them to Gauß rules. They must also be closed. An n point rule already has two of its points fixed, at the ends. The appropriate rule is known as the Gauß–Lobatto rule, which is of degree $p = 2n - 3$.

2.6 Error Analysis for the h and h - p Methods

This section is tedious, and consists mainly of technical arguments. The important parts are Theorem 2.2 on page 9; Theorem 2.3 on page 12; and the experimental results in §§2.6.3 and 2.6.4. The rest can be skipped without loss of continuity.

2.6.1 Error Analysis for the h Method

This section computes an error bound for the h method using an algebraic mesh, for the integrand $|x|^\alpha$, on $[0, 1]$. Clearly $\alpha > -1$ is necessary for the integral to be proper, and thus make its computation sensible. For $-1 < \alpha < 0$, $|x|^\alpha \notin C^0[0, 1]$, so the integrand is unbounded, but the integral is nonetheless defined. If $0 \leq \alpha < 1$, $|x|^\alpha \in C^0[0, 1]$, but $|x|^\alpha \notin C^1[0, 1]$. If $\alpha \in \mathbb{N}$, then $|x|^\alpha \in C^\infty[0, 1]$, so the singularity vanishes and the case is of lesser interest. If $\alpha > 1$, but $\alpha \notin \mathbb{N}$, then all of the higher derivatives at $x = 0$ will not exist. Using the notation $\lfloor x \rfloor$ and $\lceil x \rceil$ for the least integers (respectively) greater than and less than $x \in \mathbb{R}$, in general, for $\alpha > 1$, $|x|^\alpha \in C^{\lfloor \alpha \rfloor}[0, 1]$, but $|x|^\alpha \notin C^{\lceil \alpha \rceil}[0, 1]$. These cases are not particularly interesting, so the limit $\alpha < 1$ is made for simplicity. That is, consider $-1 < \alpha < 1$, which includes the paradigm example $x^{1/2}$. The n th derivative of $f(x) = |x|^\alpha$, for $x \neq 0$, is:

$$f^{(n)}(x) = \frac{\Gamma(\alpha + 1)}{\Gamma(\alpha + 1 - n)} |x|^{\alpha - n}.$$

Consider the interval $[0, 1]$ partitioned into m subintervals, where x_j is the j th mesh point, $j = 0 : m$, and $h_j = x_j - x_{j-1}$ is the width of the j th interval, for $j = 1 : m$. Recall, for an *algebraic* grading, a real constant $\gamma \geq 1$ is chosen,⁴ and the mesh is defined by: $x_j = (j/m)^\gamma$, $j = 0 : m$. Differentiating and applying the mean value theorem shows:

$$h_j = \left(\frac{j}{m}\right)^\gamma - \left(\frac{j-1}{m}\right)^\gamma = \frac{1}{m^\gamma} [j^\gamma - (j-1)^\gamma] \leq \frac{\gamma}{m} \left(\frac{j}{m}\right)^{\gamma-1} = \frac{dx_j}{dj}.$$

For a *geometric* grading, for some constant $0 < \sigma < 1$, $x_j = \sigma^{m-j}$, $j = 1 : m$; $x_0 = 0$, so:

$$h_j = \sigma^{m-j} - \sigma^{m-j+1} = (1 - \sigma) \sigma^{m-j}, \quad j = 2 : m, \quad h_1 = \sigma^{m-1}.$$

Consider an algebraic grading, using closed basic quadrature rules. For an h or h - p method, the integral on the j th interval is computed using a quadrature rule with $n_j \geq 2$ points. For an h method, n_j is constant; for instance, $n_j \equiv 2$ means that the integral over each mesh interval is computed using the trapezoidal rule – the rule is a *composite* trapezoidal rule. The degrees of some common quadrature rules are presented in Table 1.

Now consider the global error E_m of the difference between the true solution I and the approximation I_m , induced by the quadrature on m subintervals, that is $I = I_m + E_m$. For the function $|x|^\alpha$, bounds on E_m are readily found. Define e_j as the component of E_m due to the j th mesh interval, that is $E_m = \sum_{j=1}^m e_j$. To bound E_m , note $E_m \leq \sum_{j=1}^m |e_j|$, and then bound each of the $|e_j|$.

⁴Choosing $\gamma < 1$ results in some mesh points possibly lying outside the interval $[0, 1]$.

Degree	Gauß-Lobatto	Newton-Cotes
1	2	2 (trapezoidal)
3	3	3 (Simpson's), 4 (3/8ths)
5	4	5 (Boole's), 6
7	5	7, 8

Table 1: The number of points n , and associated degrees of some closed quadrature rules. For Gauß-Lobatto rules, the degree is $2n - 3$, and for Newton-Cotes rules, the degree is n if n is odd, else it is $n - 1$.

The error result for a degree p quadrature rule on an interval $[x_{j-1}, x_j]$, of width h_j , with a function $f(x) \in C^{p+1}[x_{j-1}, x_j]$, is:

$$e_j = C(p) h_j^{p+2} f^{(p+1)}(\xi), \quad \xi \in [x_{j-1}, x_j]. \quad (2)$$

For n point Gauß-Lobatto quadrature, the degree is $p = 2n - 3$. (2) is derived from (1) by a scaling argument, and:

$$C(p) = -\frac{(p+3)(p+5)[((p-1)/2)!]^4}{2^2(p+2)[(p+1)!]^3}. \quad (3)$$

As $|x|^\alpha \in C^\infty(0, 1]$, (2) holds for every mesh interval except the first, where the error is known exactly, e.g. for the trapezoidal rule:

$$e_1 = \frac{h_1^{\alpha+1}}{\alpha+1} - \frac{h_1}{2} h_1^\alpha = \left(\frac{1}{\alpha+1} - \frac{1}{2} \right) h_1^{\alpha+1}. \quad (4)$$

As the maximum value of the $(p+1)$ th derivative of $|x|^\alpha$ on the j th interval, is at its left hand end, $f^{(p+1)}(\xi) \leq f^{(p+1)}(x_{j-1})$, the total error can be bounded:

$$E_m \leq |e_1| + C \sum_{j=2}^m h_j^{p+2} f^{(p+1)}(x_{j-1}) \leq |e_1| + C \sum_{j=1}^{m-1} h_{j+1}^{p+2} f^{(p+1)}(x_j).$$

Here, C refers to a positive constant, independent of m , that may vary from line to line. Substituting for h_{j+1} and $f^{(p+1)}(x_j)$ using an algebraically graded mesh yields:

$$\begin{aligned} E_m &\leq |e_1| + C \sum_{j=1}^{m-1} \left[\frac{\gamma}{m} \left(\frac{j-1}{m} \right)^{\gamma-1} \right]^{p+2} \frac{\Gamma(\alpha+1)}{\Gamma(\alpha-p)} \left(\frac{j}{m} \right)^{\gamma(\alpha-p-1)} \\ &\leq |e_1| + C \sum_{j=1}^{m-1} \left[\frac{\gamma}{m} \left(\frac{j}{m} \right)^{\gamma-1} \right]^{p+2} \left(\frac{j}{m} \right)^{\gamma(\alpha-p-1)}. \end{aligned}$$

As $|e_1|$ is less than some constant multiplied by the ‘ m th term’ in the sum:

$$E_m \leq \frac{C}{m^{\gamma(\alpha+1)}} \sum_{j=1}^m j^{\gamma(\alpha+1)-(p+2)}. \quad (5)$$

Simplification of (5) (see below) leads to the result:

Theorem 2.2 (Convergence of the h Method with Algebraic Grading)

Consider the approximation of $\int_0^1 |x|^\alpha dx$, $-1 < \alpha < 1$, using an h method based on a quadrature rule of degree p (an odd positive integer), on an algebraic mesh on a total of $m \geq 2$ intervals, with mesh parameter $\gamma \geq 1$. For some constant C , the error E_m satisfies:

$$E_m \leq C m^{-z}.$$

Here z is:

$$z = \begin{cases} \gamma(\alpha + 1) & 1 \leq \gamma < (p + 1) / (\alpha + 1) \\ p + 1 & \text{else.} \end{cases}$$

When $\gamma = (p + 1) / (\alpha + 1)$, $E_m \leq C \ln(m) / m^{p+1}$.

Theorem 2.1 Take (5) and write E_m as:

$$\begin{aligned} E_m &\leq \frac{C}{m^{\gamma(\alpha+1)}} \sum_{j=1}^m j^{\gamma(\alpha+1)-(p+2)} \leq \frac{C}{m^{\gamma(\alpha+1)}} \int_1^m x^{\gamma(\alpha+1)-(p+2)} dx \\ &\leq \frac{C}{m^{\gamma(\alpha+1)}} \int_1^\infty x^{\gamma(\alpha+1)-(p+2)} dx. \end{aligned}$$

The integral converges if: $\gamma(\alpha + 1) - (p + 2) < -1$, and in this case, it converges to the constant $[(p + 1) - \gamma(\alpha + 1)]^{-1}$, independent of m . Absorbing this into the main constant, the result for $1 \leq \gamma < (p + 1) / (\alpha + 1)$ is created.

In the case $\gamma = (p + 1) / (\alpha + 1)$, (5) is

$$E_m \leq \frac{C}{m^{p+1}} \sum_{j=1}^m \frac{1}{j} \leq \frac{C}{m^{p+1}} \int_1^m \frac{1}{x} dx \leq \frac{C}{m^{p+1}} \ln(m).$$

Thus again, the error is bounded by a constant, this time, dependent on m . Observe that $p + 1$ is immediately able to be replaced with $\gamma(\alpha + 1)$, demonstrating the continuity of the formulae.

Lastly, bound E_m as:

$$\begin{aligned} E_m &\leq \frac{C}{m^{p+2}} \sum_{j=1}^m \left(\frac{j}{m}\right)^{\gamma(\alpha+1)-(p+2)} \leq \frac{C}{m^{p+2}} \int_{1/m}^1 x^{\gamma(\alpha+1)-(p+2)} dx \\ &\leq \frac{C}{m^{p+2}} \int_0^1 x^{\gamma(\alpha+1)-(p+2)} dx. \end{aligned}$$

As $\gamma(\alpha + 1) - (p + 2) > -1$, the integral converges to $[\gamma(\alpha + 1) - (p + 1)]^{-1}$, again, another constant independent of m , which is absorbed into C . The second result is thus achieved, by observing that $m^{-(p+2)} < m^{-(p+1)}$.

The moral of this is that for a particular choice of α and p , there is an ideal choice of γ , that is $\gamma^* = (p + 1) / (\alpha + 1)$, beyond which the order of the error will not decrease. (Choosing γ greater than this may reduce C .) Varying γ makes no difference to computational expense.⁵ Observe that γ^* becomes unbounded as $\alpha \rightarrow -1^+$.

⁵Choosing $\lceil \gamma^* \rceil$ may be cheaper than nonintegral choices of γ^* .

This is not surprising, as the integral itself becomes unbounded. A similar result to Theorem 2.2 exists for a geometric mesh.

In summary, using an algebraic mesh of m subintervals, and an h method with a degree p quadrature rule on each mesh interval, can achieve, for $|x|^\alpha$ integrands, an $\mathcal{O}(m^{-(p+1)})$ convergence rate. This is a significant improvement on the equivalent result for a uniform mesh, which is $\mathcal{O}(m^{-(\alpha+1)})$. The exponential convergence rate for smooth integrands is not achieved, but can be, using an h - p method. The methods may be extended to integrands of the form $|x|^\alpha f(x)$, for smooth functions f .

2.6.2 Error Analysis for the h - p Method

This section discusses the expected order of the error for the h - p method, for algebraic or geometric meshes using integrands with end point singularities. Again, consider the integral $\int_0^1 |x|^\alpha dx$. For the h method, p_j , the degree of the quadrature rule on the j th interval, was constant. For the h - p method, it is a function of j . A low degree rule is used on the interval adjacent to the end point singularity; and higher degree rules are used on intervals away from it. A simple choice is to use a rule on 2 points on the first interval, and increase the number of points linearly with j . That is, using Gauß–Lobatto rules, where $p_j = 2n_j - 3$; choosing $n_j = j + 1$ gives $p_j = 2j - 1$.

Recall the error result from (2), where $C_j = C(p_j)$ is given by (3):

$$\int_{x_{j-1}}^{x_j} f(x) dx - I_{p_j} = e_j = C_j h_j^{p_j+2} f^{(p+1)}(\xi), \quad \xi \in [x_{j-1}, x_j].$$

Use Stirling's formula for large x to approximate the factorials in C_j , as $(x-1)! = \Gamma(x)$:

$$\Gamma(x) \sim \sqrt{\frac{2\pi}{x}} \left(\frac{x}{e}\right)^x \left\{1 + \frac{1}{12x} + \dots\right\}.$$

Applying the first term of this to (3) gives an asymptotic bound for large j :

$$C_j = -\frac{(j+1)(j+2)}{2j+1} \frac{[(j-1)!]^4}{[(2j)!]^3} \sim -\frac{2^7}{e^3} \sqrt{\pi j} \left(\frac{e}{8j}\right)^{2j+3}.$$

Thus:

$$|C_j| \leq C \frac{\mu^j}{j^{5/2+2j}}, \quad \mu = e^2/2^6. \quad (6)$$

E_m cannot be bounded directly using this approximation for C_j , as it is not a proper bound. Heuristically,⁶ for either a geometric or an algebraic mesh, the rapid convergence of C_j to 0 means that E_m is expected to be dominated by e_1 . Consider a mesh on m intervals, and an associated composite quadrature rule on a total of $N = m(m+1)/2 + 1$ points. For a geometric mesh $h_1 = \sigma^{m-1}$, and for an algebraic mesh $h_1 = m^{-\gamma}$. Using (4), this gives:

$$|e_1| \leq C h_1^{\alpha+1} \leq C \begin{cases} m^{-\gamma(\alpha+1)} & \text{algebraic} \\ \sigma^{(m-1)(\alpha+1)} & \text{geometric.} \end{cases} \quad (7)$$

⁶This is brought out by experiment.

The error for an algebraic mesh is polynomial, whilst the error for a geometric mesh is exponential. If the errors with increasing $N \approx m^2/2$ are plotted for a geometric mesh, an error of the form $E_m \leq C\rho^{\sqrt{N}}$ is observed (see Figure 2), for some $\rho < 1$.

These rough results prompt more rigorous examination of E_m . Recall:

$$|e_j| \leq C_j h_j^{2j+3} f^{(2j+2)}(x_{j-1}).$$

For a geometric mesh, $x_j = \sigma^{m-j}$, so $h_j < (1 - \sigma)\sigma^{m-j}$. Using $f(x) = |x|^\alpha$, gives:

$$f^{(n)}(x) = \frac{\Gamma(\alpha + 1)}{\Gamma(\alpha + 1 - n)} |x|^{\alpha - n}.$$

The Stirling asymptotic approximation for C_j can be converted to a genuine bound by observing for $x \in \mathbb{N}$:

$$\sqrt{\frac{2\pi}{x}} \left(\frac{x}{e}\right)^x \leq \Gamma(x) \leq C \sqrt{\frac{2\pi}{x}} \left(\frac{x}{e}\right)^x.$$

Recall from (6), that with $\mu = e^2/2^6$, for some C independent of x :

$$|C_j| \leq C \frac{\mu^j}{j^{2j+5/2}}.$$

A bound on the error for the j th interval is now:⁷

$$|e_j| < C \frac{\mu^j}{j^{2j+5/2}} [(1 - \sigma)\sigma^{m-j}]^{2j+3} f^{(2j+2)}(\sigma^{m-j-1}).$$

Simplification of this leads to a bound on E_m . Observe that $(1 - \sigma)^{2j+3} < 1$, so:

$$|e_j| < C \frac{\mu^j}{j^{2j+5/2}} \sigma^{(m-j)(2j+3)} \frac{\Gamma(\alpha + 1)}{\Gamma(\alpha - 2j - 1)} \sigma^{(m-j-1)(\alpha - 2j - 2)}.$$

Absorb $\Gamma(\alpha + 1)$ into C , and use the Stirling approximation for $\Gamma(\alpha - 2j - 1)$:

$$\frac{1}{\Gamma(\alpha - 2j - 1)} \leq \sqrt{\frac{\alpha - 2j - 1}{2\pi}} \left(\frac{e}{\alpha - 2j - 1}\right)^{\alpha - 2j - 1}.$$

Rearranging the exponent of σ , and absorbing the term $e^{\alpha-1}$ into C :

$$\begin{aligned} |e_j| &< C \frac{\mu^j}{j^{2j+5/2}} \sigma^{(m-j)(\alpha+1) - \alpha + 2j+2} \sqrt{\frac{\alpha - 2j - 1}{2\pi}} \left(\frac{e}{\alpha - 2j - 1}\right)^{\alpha - 2j - 1} \\ &< C \frac{\mu^j \sigma^{m(\alpha+1)} \sigma^{j(1-\alpha)} e^{-2j}}{j^{2j+5/2} (\alpha - 2j - 1)^{\alpha - 2j - 1/2}}. \end{aligned}$$

Expand $\mu = e^2/2^6$, and observe that $(\alpha - 2j - 1)^{\alpha - 1/2} > 1$:

$$|e_j| < C \frac{e^{2j} \sigma^{m(\alpha+1)} \sigma^{j(1-\alpha)} e^{-2j}}{j^{2j+5/2} 2^{6j} (\alpha - 2j - 1)^{-2j}} < C \frac{\sigma^{m(\alpha+1)} \sigma^{j(1-\alpha)}}{2^{6j} j^{5/2}} \left(\frac{\alpha - 2j - 1}{j}\right)^{2j}.$$

As $|(\alpha - 2j - 1)/j| < 2$, then:

$$|e_j| < C \frac{2^{2j} \sigma^{m(\alpha+1)} \sigma^{j(1-\alpha)}}{2^{6j} j^{5/2}} < C \frac{\sigma^{m(\alpha+1)} \sigma^{j(1-\alpha)}}{2^{4j} j^{5/2}}.$$

⁷Strictly speaking, this only applies for $j = 2 : m$, as the result for C_j only holds for $j = 2 : m$. Application of the result in (7) allows $|e_1|$ to be bounded by a constant multiple of this C_1 .

Combine these, to bound:

$$E_m \leq \sum_{j=1}^m |e_j| < C \sum_{j=1}^m \frac{\sigma^{m(\alpha+1)} \sigma^{j(1-\alpha)}}{2^{4j} j^{5/2}} < C \sigma^{m(\alpha+1)} \sum_{j=1}^m \frac{\sigma^{j(1-\alpha)}}{2^{4j} j^{5/2}}.$$

Observing that $2^{4j} j^{5/2} > 1$, this can be written as:⁸

$$E_m < C \sigma^{m(\alpha+1)} \sum_{j=1}^m \left[\sigma^{(1-\alpha)} \right]^j.$$

Using the result for the sum of a geometric progression:

$$\sum_{j=1}^m \left[\sigma^{(1-\alpha)} \right]^j = \frac{(\sigma^{1-\alpha})^{m+1} - 1}{\sigma^{1-\alpha} - 1} = \frac{\sigma^{(1-\alpha)(m+1)} - 1}{\sigma^{1-\alpha} - 1} < C \sigma^{(1-\alpha)(m+1)}.$$

Thus: $E_m < C \sigma^{m(\alpha+1)} \sigma^{(1-\alpha)(m+1)} < C \sigma^{2m}$. As $N \approx m^2/2$, using $\rho = \sigma^{2\sqrt{2}}$, this simplifies to:

$$E_m < C \rho^{\sqrt{N}}.$$

This constant C is actually a function of α and σ , and the fact that the degrees of the quadrature rules are linearly graded. This proves Theorem 2.3:

Theorem 2.3 (Convergence of the h - p Method with Geometric Grading)

Consider the approximation of $\int_0^1 |x|^\alpha dx$, $-1 < \alpha < 1$, using an h - p method based on a geometric mesh on m intervals with parameter σ , and using a Gauß–Lobatto quadrature rule on $j + 1$ points on interval j . For some constants C , and $\rho < 1$, the error E_m satisfies:

$$E_m < C \sigma^{2m}.$$

Babuška et al. [1, 12, 13, 14] describe an approximation theory for the h , p and h - p methods for the finite element method. This material may be able to be simplified and adapted (as the theory for integration should be easier than for approximation), and also used in error analysis.

2.6.3 Experimental Results for a Real Integral

The example $\int_0^1 \sqrt{x} dx$ is used to demonstrate the above convergence results. MATLAB code used (`hpmeth.m` and `funchp.m`), is contained in Appendix A, and error results are presented in Figures 1 and 2.

Figure 1 compares convergence rates for various choices of the algebraic grading parameter γ , whilst holding constant the number of points in the quadrature rule used on each interval; that is $p = 6$ is fixed. Figure 2 shows similar data, but varies p . (Here, γ is allowed to vary, and is chosen to be equal to p for convenience.) Both plots are shown compared with the corresponding h - p result, using a geometric grading, and $\sigma = 0.15$. The linear increase in number of points used in the quadrature rule means that $n_j = j + 1$, $j = 1 : m$, so $N = m(m + 1)/2 + 1$ (as rules are closed, but ends are not), and thus $m \propto \sqrt{N}$. The h - p result demonstrates $\mathcal{O}(\rho^{\sqrt{N}})$ behaviour. The h - p data does not show as a straight line, but this can be seen in Figure 3, where it is plotted versus \sqrt{N} .

⁸This throws away a lot of information!

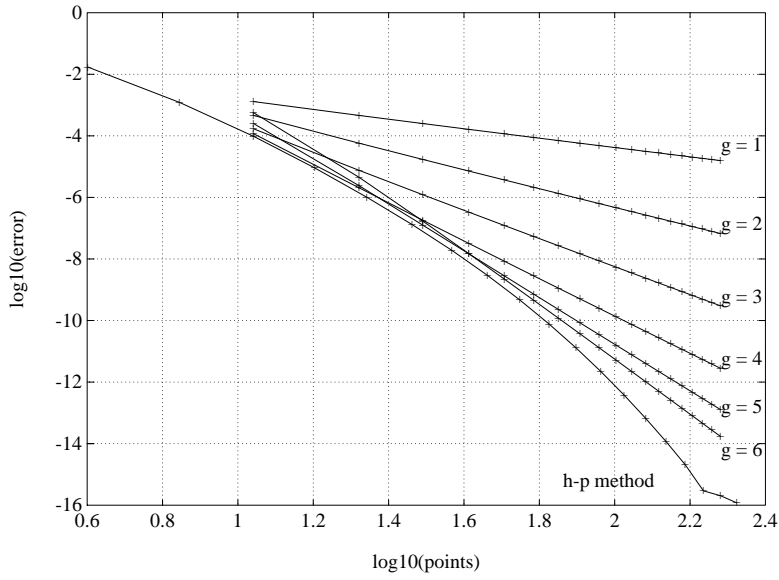


Figure 1: Errors for h and h - p methods applied to $\int_0^1 \sqrt{x} dx$, for various choices of $\gamma \equiv g$. The slopes of the lines are approximately $-3\gamma/2$. As the error tends to machine precision ($\epsilon \approx 10^{-16}$), the convergence results lose their regularity.

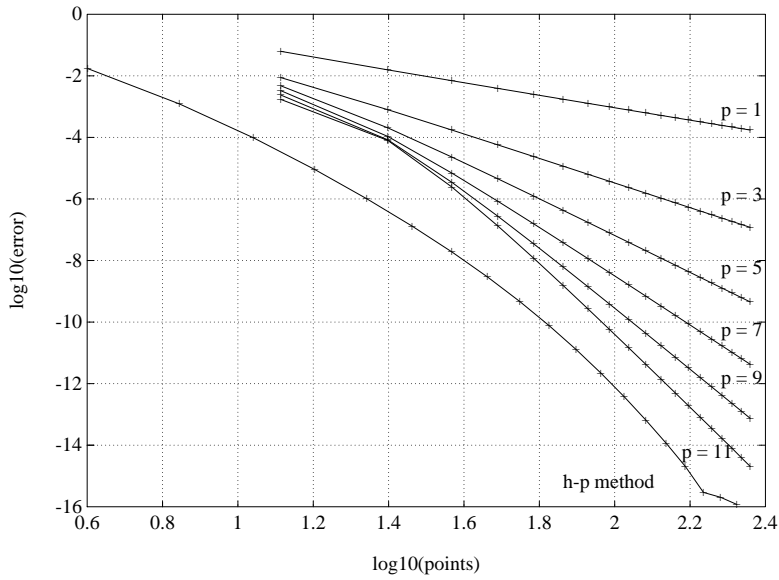


Figure 2: Errors for h and h - p methods applied to $\int_0^1 \sqrt{x} dx$, for constant p . The slopes of the lines are approximately $-(p+1)$.

2.6.4 Extension to Complex Contour Integrals

The method is easily extended to complex contour integrals. Good test problems have closed contours, and integrals which can be directly evaluated using Cauchy's integral formula. To demonstrate this, consider $f(z) = e^{-i\pi/4} z^{-1} \sqrt{z-1}$, integrated around the unit circle. The integrand has a simple pole at $z = 0$, and a derivative singularity at $z = 1$. The resulting integral is:

$$\oint_{\Gamma} f(z) dz = e^{i\pi/4}.$$

MATLAB code used (`cint.m` and `funcci.m`) is contained in Appendix A. Error results for an h - p method using Gauß-Lobatto quadrature rules are presented in Figure 3. The mesh is geometrically graded, with parameter $\sigma = 0.15$. For a segment of a closed contour, with a corner at either end, let D be chosen as the number of mesh intervals between each corner and a wide, central interval, so $m = 2D + 1$ is the number of mesh intervals over that segment. Here, as the contour is the unit circle, 2 artificial corners are placed, and D is varied from 8 to 15. The grading of the quadrature rules is similar to that used in §2.6.3 – the number of points used in the quadrature rule increases linearly with the number of mesh intervals from the nearest corner, starting at 2 on the interval nearest the corner, and finishing at $D + 2$ on the central interval.

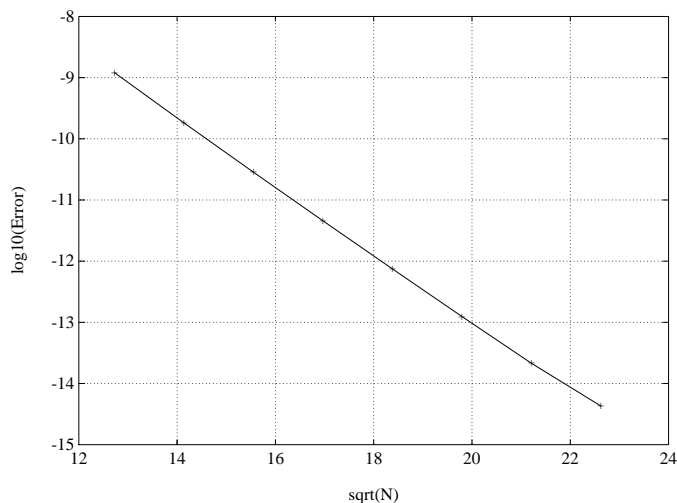


Figure 3: Error results for the complex contour integral.

Convergence is plotted for the logarithm of the error with \sqrt{N} . Observe that the plot is linear, that is, the error is $\mathcal{O}(\rho^{\sqrt{N}})$. These superb results show that the method is excellent for the numerical approximation of closed complex contour integrals. This success motivates the use of the h - p method in the CBIEM, where quadrature rules for complex contour integrals are required in the numerical approximation of the solution to an integral equation.

2.7 Summary – Advantages of h - p Methods

This section has discussed three important aspects of the numerical approximation of integrals with end point singularities:

1. An h - p quadrature method is superior to other methods.
2. A geometrically graded mesh is superior to other choices of grading (maybe only marginally better than an algebraic one).
3. The appropriate family of quadrature rules to use is the Gauß–Lobatto, as they are closed, and of maximal degree for the number of quadrature points used.

The quadrature rule used in §3 is chosen in this manner.

3 The Complex Boundary Integral Equation Method

3.1 Origins and Description

The CBIEM is a technique which numerically approximates the solution of the Dirichlet problem.⁹ It reformulates the solution of the Dirichlet problem as the real part of a function which can be found as the solution of a complex boundary integral equation. The solution of a discretised version of this integral equation is then found using a collocation technique. Finally, a discretisation of Cauchy’s integral formula is used to approximate the solution to the original problem at interior points, based on the approximate boundary data.

It is related to the ‘Complex Variable Boundary Element Method’ [15], which is a Galerkin version of the same technique, using ‘hat’ functions as a basis. (The collocation method creates an approximation to the boundary data by interpolating from known data, whilst the Galerkin constructs an approximation in terms of a series of basis functions defined on segments of the boundary.) As originally stated, the CVBEM only works on polygonal domains,¹⁰ whilst the CBIEM is more general in that it also works on non-polygonal domains.

The Dirichlet problem considered is on an open, finite, simply connected and non-empty region $\Omega \subset \mathbb{R}^2$. Ω is bounded by Γ , a piecewise continuous, anticlockwise oriented contour. Γ has a finite number of corners, at which its derivative is discontinuous. The Dirichlet problem is:

Given boundary data f , find $U : \Omega \mapsto \mathbb{R}$ subject to the conditions:

$$\nabla^2 U(\mathbf{x}) = 0, \quad \mathbf{x} \in \Omega, \quad U(\mathbf{x}) = f(\mathbf{x}), \quad \mathbf{x} \in \Gamma.$$

Thus, the problem is to find the solution to Laplace’s equation over a region, given functional data around its perimeter. This has many applications in the solution of potential problems, such as electrostatics and fluid flow. The value of U at points interior to Ω is determined by the boundary data being ‘diffused’ from the boundary inwards, according to the Laplacian operator. It turns out that the problem has a unique solution for all cases of f . In all but the most trivial cases, this solution is not expressible in closed form, and a numerical approximation is required. With sufficient (possibly enormous) computational effort, an approximation to any degree of accuracy can usually be obtained.

Problems with ‘corner singularities’ are of particular interest. In these problems, U is differentiable in the interior, but ∇U becomes unbounded as the corner is approached. It is known that this behaviour is typical of solutions to the Dirichlet problem on domains with corners. Even if the boundary data is smooth, ∇U still becomes singular near the corner. Numerical methods must be able to produce good approximations to U , in spite of the corner singularities.

‘Interior’ methods, such as finite difference and finite element methods, become computationally expensive when applied to problems with corner singularities, and boundary integral methods are more appropriate. Interior methods require a finely discretised two dimensional mesh in the region of the corner, which greatly increases the size of the associated linear system. In contrast, a boundary integral method has only to discretise its mesh in one dimension, that of arc length on the boundary, and is expected to be much cheaper.

⁹The space containing the functions approximating the solution of the Dirichlet problem is a Sobolev space, which is a generalisation of the Banach space of continuous functions to include functions with ‘weak derivatives’.

¹⁰The CVBEM has also been generalised to doubly connected domains [18].

The usual boundary integral methods based on Green's functions lead to a kernel with a logarithmic singularity, even on a smooth domain. This is tedious to program, and computationally inefficient if high order methods are used. If the CBIEM is used with singularity subtraction, the integrands are smooth and can be done simply and accurately by direct quadrature.

The problems caused by the corners and corner singularities are dealt with using h - p quadrature methods, and would be difficult to implement with other types of integral equations [3].

3.2 Development of the CBIEM

The solution to the Dirichlet problem, U , is harmonic, as it satisfies Laplace's equation in Ω . Identify $\mathbf{x} \in \mathbb{R}^2$ with $z \in \mathbb{C}$. Now U can be thought of as the real component of an analytic function $W(z) = U(z) + iV(z)$, where V is uniquely determined to within a constant. V can be made unique by requiring $V(\zeta_0) = 0$ for some $\zeta_0 \in \Gamma$ (see §3.2.5). For all $z \in \Gamma$, $U(z) \equiv f(z)$ is immediately known. The CBIEM first approximates $V(z)$ on Γ , and then uses Cauchy's integral formula to approximate W , and hence U , at points within Ω .

3.2.1 Cauchy's Integral Formula

For an analytic function W on a bounded domain Ω , Cauchy's integral formula is:

$$\oint_{\Gamma} \frac{W(\zeta)}{\zeta - z} d\zeta = \pi i W(z) \times \begin{cases} 0 & z \notin \Omega \cup \Gamma & \text{exterior} \\ 1 & z \in \Gamma & \text{boundary} \\ 2 & z \in \Omega & \text{interior.} \end{cases} \quad (8)$$

When z is on the boundary,¹¹ the integral is a Hilbert transform. The kernel is singular, and the result must be interpreted as a Cauchy principal value integral [2, page 39]. The CBIEM requires approximation of the Cauchy integrals by quadrature. In §3.2.3, this is used to set up a linear system for the approximation of V on Γ . After this has been done, in §3.3 it is used to compute an approximation to W (and hence U) in the interior of Ω .

3.2.2 The Complex Boundary Integral Equation

To derive the integral equation underlying the CBIEM, observe that letting $W(\zeta) \equiv 1$ for the case $z \in \Gamma$ in (8) yields:

$$\oint_{\Gamma} \frac{1}{\zeta - z} d\zeta = \pi i, \quad z \in \Gamma.$$

Multiplying this by the constant $W(z)$ gives:

$$W(z) \oint_{\Gamma} \frac{1}{\zeta - z} d\zeta = \oint_{\Gamma} \frac{W(z)}{\zeta - z} d\zeta = \pi i W(z).$$

Equating the $\pi i W(z)$ with that in (8) gives:

$$\oint_{\Gamma} \frac{W(\zeta) - W(z)}{\zeta - z} d\zeta = 0, \quad z \in \Gamma. \quad (9)$$

(9) is called the 'Complex Boundary Integral Equation'. This derivation is parallel to that involved in *singularity subtraction* [6, page 184] and [4]. The integrand is analytic, and as $\zeta \rightarrow z$, it converges to $W'(z)$. An analytic function $W = U + iV$, which has as its real component the solution to the Dirichlet problem, will satisfy (9). The converse is also true – a function W that satisfies (9) will have a real component U that satisfies the Dirichlet problem. It is hoped that a function that satisfies a discretisation of (9) will have as its real part the solution to a discretisation of the Dirichlet problem.

¹¹This result is a simplification. If z is at a corner, replace 1 with α/π , where α is the interior angle subtended by the corner (else $\alpha = \pi$). This result requires that collocation points are *not* placed at corners, to avoid unwanted complexities in the implementation. Fortunately, this is already overcome by the use of node points at the corners (see §3.2.3).

3.2.3 Discretisation of the CBIE

The CBIEM requires the numerical approximation of the (Cauchy) integral in (9), and this is achieved using quadrature. In particular, given the possibly singular nature of W at corners, §2 motivates the use of geometrically graded h - p quadrature, because it is of high order for such integrands. The approximation will be referred to as a discretisation. Nomenclature used in the following discussion is shown in Figure 4. (The distinction between *mesh* and *node* (quadrature) points is made in §2.5.3.)

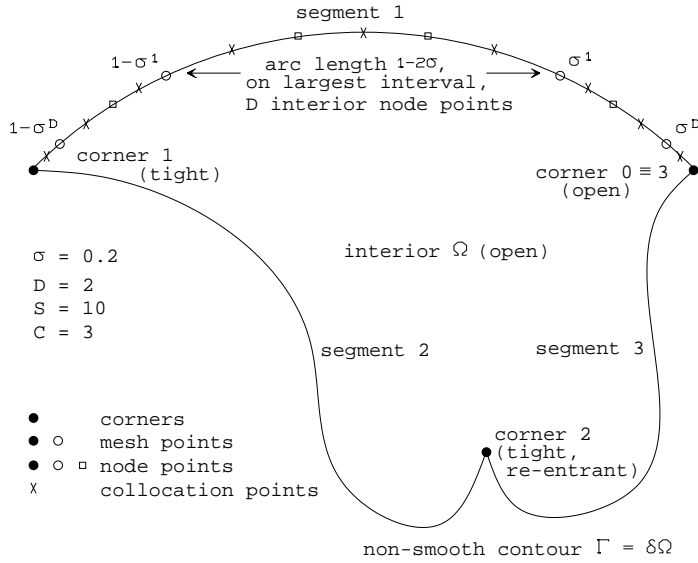


Figure 4: CBIEM nomenclature. Corner, mesh, node and collocation points on contour Γ , about a region Ω . The lengths marked on segment 1 are the positions of geometric mesh points, in terms of a unit arc length on that segment. The node points correspond to a closed Newton–Cotes rule on each mesh interval.

Consider the contour integral of an arbitrary integrand $g(\zeta)$ around Γ :

$$\oint_{\Gamma} g(\zeta) d\zeta.$$

Parameterise Γ using $\gamma : [0, 1] \mapsto \mathbb{C}$, such that $\zeta_0 \equiv \gamma(0) = \gamma(1) \equiv \zeta_N$, with argument t increasing in an anticlockwise direction around Γ . The contour integral is [6, page 168]:¹²

$$\oint_{\Gamma} g(\zeta) d\zeta = \int_0^1 g(\gamma(t)) \frac{\partial \gamma}{\partial t}(t) dt.$$

¹²This requires that γ is continuous, and that $\gamma|_{[t_{i-1}, t_i]}$ is continuously differentiable for a finite partition $0 = t_0 < t_1 < \dots < t_n = 1$.

Approximate the integral using an h - p quadrature rule $\{t_j, w_j\}$ with N node points, defining $\zeta_j = \gamma(t_j)$ and $\dot{\gamma}_j = \frac{\partial \gamma}{\partial t}(t_j)$:

$$\oint_{\Gamma} g(\zeta) d\zeta = \int_0^1 g(\gamma(t)) \frac{\partial \gamma}{\partial t}(t) dt \approx \sum_{j=1}^N g(\zeta_j) \dot{\gamma}_j w_j.$$

This formula can be applied to the Cauchy integrals. For some fixed $z \in \Gamma$, consider the integrand $g(\zeta) = (W(\zeta) - W(z))/(\zeta - z)$. Let $W_j = W(\zeta_j)$, and redefine $w_j \leftarrow \dot{\gamma}_j w_j$ to absorb $\dot{\gamma}_j$. The Cauchy integral is:

$$\oint_{\Gamma} \frac{W(\zeta) - W(z)}{\zeta - z} d\zeta \approx \sum_{j=1}^N \frac{W_j - W(z)}{\zeta_j - z} w_j, \quad z \in \Gamma. \quad (10)$$

Approximation of the solution to the CBIE requires approximation of the Cauchy integrals without using $W(z)$. Instead, $\hat{W}(z) \approx W(z)$ is constructed from values of W at the quadrature points. (10) is discretised into a linear system of order N .

Begin by choosing a set of N different values of z from around the boundary. These points are called the *collocation* points. It is known from analysis in the case of uniform meshes that collocation points must not lie on node points [20]. The natural choice is to take as the collocation points the N midpoints (in the sense of arc length) between the N node points.¹³ Let $t_{k-1/2} = (t_{k-1} + t_k)/2$, $\zeta_{k-1/2} = \gamma(t_{k-1/2})$ and $W_{k-1/2} = W(\zeta_{k-1/2})$, for $k = 1 : N$. Interpolation from known values of U at the node and collocation points is used with the CBIE to approximate the $W_{k-1/2}$.

Define two complex N -vectors of W at the node and collocation points:

$$\mathbf{W} = \begin{bmatrix} W_1 \\ \vdots \\ W_N \end{bmatrix}, \quad \mathbf{W}' = \begin{bmatrix} W_{1/2} \\ \vdots \\ W_{N-1/2} \end{bmatrix}.$$

Also define the real N -vectors $\mathbf{U} = \Re(\mathbf{W})$, $\mathbf{U}' = \Re(\mathbf{W}')$ and $\mathbf{V} = \Im(\mathbf{W})$. From (10), an order N linear system for the components of \mathbf{W} and \mathbf{W}' is determined:

$$\sum_{j=1}^N \frac{W_j - W_{k-1/2}}{\zeta_j - \zeta_{k-1/2}} w_j = 0, \quad k = 1 : N. \quad (11)$$

In summary, discretisation of Cauchy's integral formula leads to a linear system, the solution to which is an approximation to W at the N node points on Γ . This approximation can be used to approximate W , and hence U , at points within Ω .

¹³The choice $\zeta_{k-1/2} = (\zeta_{k-1} + \zeta_k)/2$ is explicitly *not* used, as this assumes the contour is linear between points parameterised by t_{k-1} and t_k .

3.2.4 Linear Interpolation of W at the Collocation Points

If the W_j were known, (11) could be directly used to interpolate the $W_{k-1/2}$. However, although U_j and $U_{k-1/2}$ are known explicitly, V_j and $V_{k-1/2}$ are not. The CBIEM implicitly approximates the $V_{k-1/2}$ by interpolation from the as yet undetermined V_j at points near $\zeta_{k-1/2}$. That is, if a rule on O points is being used, choose O terms from the sequence:

$$\dots, \zeta_{k-3}, \zeta_{k-2}, \zeta_{k-1}; \zeta_k, \zeta_{k+1}, \zeta_{k+2}, \dots$$

The discretisation of the CBIE in (11), coupled with the $2N$ knowns U_j and $U_{k-1/2}$, and the interpolation for the $V_{k-1/2}$, allows the approximation of the N unknowns V_j . (The $V_{k-1/2}$ are *not* explicitly required to be calculated.)

The simplest interpolation for the $V_{k-1/2}$ is a linear one, between ζ_{k-1} and ζ_k , that is use:

$$V_{k-1/2} \approx (V_{k-1} + V_k)/2. \quad (12)$$

More sophisticated interpolations to the $V_{k-1/2}$ could involve higher degree polynomials, splines, or trigonometric polynomials. Initially, the linear choice will be used to illustrate the process. In §3.5.1, the method is extended to higher degree polynomials. For a particular problem (Ω, f) , there is an optimal choice of degree for the interpolation, as errors incurred by interpolation increase with the degree, and eventually become of greater magnitude than those due to discretisation.

The W_j are found by solving for their imaginary parts V_j , and combining these with the knowns U_j . The linear system is set up as follows. Substituting $W_j = U_j + iV_j$ and $W_{k-1/2} = U_{k-1/2} + iV_{k-1/2}$ into (11), using (12), and collecting knowns and unknowns:

$$\sum_{j=1}^N \frac{\frac{1}{2}V_{k-1} + \frac{1}{2}V_k - V_j}{\zeta_j - \zeta_{k-1/2}} w_j = i \sum_{j=1}^N \frac{U_{k-1/2} - U_j}{\zeta_j - \zeta_{k-1/2}} w_j, \quad k = 1 : N. \quad (13)$$

This is a system of N equations for the N unknowns V_j , with RHS determined by the knowns U_j and $U_{k-1/2}$ (and of course the associated ζ_j and $\zeta_{k-1/2}$).

3.2.5 Solution of the Collocation Equations

In order to write (13) as a linear system, consider the LHS of its k th equation:

$$\frac{1}{2}V_{k-1} \sum_{j=1}^N \frac{w_j}{\zeta_j - \zeta_{k-1/2}} + \frac{1}{2}V_k \sum_{j=1}^N \frac{w_j}{\zeta_j - \zeta_{k-1/2}} - \sum_{j=1}^N \frac{V_j w_j}{\zeta_j - \zeta_{k-1/2}}. \quad (14)$$

Define a matrix $A \in \mathbb{C}^{N \times N}$:

$$A = \begin{bmatrix} \frac{w_1}{\zeta_1 - \zeta_{1/2}} & \frac{w_2}{\zeta_2 - \zeta_{1/2}} & \cdots & \frac{w_N}{\zeta_N - \zeta_{1/2}} \\ \frac{w_1}{\zeta_1 - \zeta_{3/2}} & \frac{w_2}{\zeta_2 - \zeta_{3/2}} & \cdots & \frac{w_N}{\zeta_N - \zeta_{3/2}} \\ \vdots & \vdots & \ddots & \vdots \\ \frac{w_1}{\zeta_1 - \zeta_{N-1/2}} & \frac{w_2}{\zeta_2 - \zeta_{N-1/2}} & \cdots & \frac{w_N}{\zeta_N - \zeta_{N-1/2}} \end{bmatrix}.$$

Also define a set of N scalars H_k , for $k = 1 : N$ (the row sums of A):

$$H_k = \sum_{j=1}^N \frac{w_j}{\zeta_j - \zeta_{k-1/2}}.$$

The first two terms of (14) are then $\frac{1}{2}V_{k-1}H_k + \frac{1}{2}V_kH_k$. As Γ is closed, $\zeta_0 \equiv \zeta_N$ and hence $V_0 = V_N$. Define $B \in \mathbb{C}^{N \times N}$:

$$B = \frac{1}{2} \begin{bmatrix} H_1 & & & & & & & H_1 \\ H_2 & H_2 & & & & & & \\ & \ddots & \ddots & & & & & \\ & & & H_{N-1} & H_{N-1} & & & \\ & & & & H_N & H_N & & \end{bmatrix}. \quad (15)$$

Let $C = B - A$, then the LHS of (13) is $C\mathbf{V}$. Let $\mathbf{1}_N \in \mathbb{R}^N$ represent the real column vector with all components unity, and the operation $\text{diag}(\mathbf{x})$ on N -vector \mathbf{x} create the diagonal matrix of order N with the diagonal entries being the respective components of \mathbf{x} . Defining $\mathbf{d} = \text{diag}(A\mathbf{1}_N)\mathbf{U}' - A\mathbf{U}$, the system for \mathbf{V} is:

$$C\mathbf{V} = i\mathbf{d}. \quad (16)$$

Attempting to directly solve the complex linear system in (16) fails, as \mathbf{V} is overdetermined in two separate ways. Firstly, \mathbf{V} is purely real, that is $\Im(\mathbf{V}) = \mathbf{0}$. Partitioning (16) into real and imaginary components yields two purely real linear systems, either one of which can be solved for what should be the same solution $\hat{\mathbf{V}}$. The system to be solved is: $\Re(C)\mathbf{V} = -\Im(\mathbf{d})$ or $\Im(C)\mathbf{V} = \Re(\mathbf{d})$. By redefining $C \leftarrow \Re(C)$ and $\mathbf{d} \leftarrow -\Im(\mathbf{d})$, the first choice for the solution of \mathbf{V} is made. The linear system is thus:

$$C\mathbf{V} = \mathbf{d}. \quad (17)$$

The second way that (16) is overdetermined is that \mathbf{V} is known only to within a constant.¹⁴ So, if direct solution of (17) is attempted, singularity problems will occur, and the resultant $\hat{\mathbf{V}}$ will be infinite.¹⁵ To accommodate this, arbitrarily¹⁶ set $V_N = 0$, and compute the rest of the components of \mathbf{V} by subtracting rows in (17). The result is a fully determined order $N - 1$ linear system. The N rows of (17) are:

$$(C\mathbf{V})_j = \mathbf{d}_j, \quad j = 1 : N.$$

Subtracting rows gives a system of $N - 1$ equations:

$$(C^*\mathbf{V})_{j-1} = (C\mathbf{V})_j - (C\mathbf{V})_{j-1} = \mathbf{d}_j - \mathbf{d}_{j-1} = \mathbf{d}_{j-1}^*, \quad j = 2 : N.$$

Defining $\mathbf{V}^* \in \mathbb{R}^{N-1}$ as the first $N - 1$ entries of \mathbf{V} (where the last entry is zero):

$$C^*\mathbf{V}^* = \mathbf{d}^*. \quad (18)$$

Here:

$$C^* = \begin{bmatrix} C_{2,1} - C_{1,1} & \cdots & C_{2,N-1} - C_{1,N-1} \\ C_{3,1} - C_{2,1} & \cdots & C_{3,N-1} - C_{2,N-1} \\ \vdots & \ddots & \vdots \\ C_{N,1} - C_{N-1,1} & \cdots & C_{N,N-1} - C_{N-1,N-1} \end{bmatrix} \in \mathbb{R}^{(N-1) \times (N-1)}$$

$$\mathbf{d}^* = \begin{bmatrix} d_2 - d_1 \\ d_3 - d_2 \\ \vdots \\ d_N - d_{N-1} \end{bmatrix} \in \mathbb{R}^{N-1}.$$

Solution of the order $N - 1$ linear system in (18) yields the approximation to \mathbf{V} , and hence \mathbf{W} (W at the N node points).

¹⁴A scalar multiple of $\mathbf{1}_N$.

¹⁵Well, a numerical approximation to ∞ !

¹⁶For test problems, $\hat{V}_N = V(\zeta_N)$ is actually used.

3.3 Approximation of U at Interior Points

The approximation $\mathbf{W} = \mathbf{U} + i\mathbf{V}$ on Γ is used to approximate W (and hence U) at interior points of Ω , using Cauchy's integral formula for points within Ω :

$$W(z) = \frac{1}{2\pi i} \oint_{\Gamma} \frac{W(\zeta)}{\zeta - z} d\zeta, \quad z \in \Omega.$$

Discretising this gives the approximation, for $z \in \Omega$:

$$W(z) \approx \frac{1}{2\pi i} \sum_{j=1}^N \frac{W(\zeta_j)}{\zeta_j - z} w_j. \quad (19)$$

Numerical problems occur using this simple approximation, as points $z \in \Omega$ near the boundary (where $z - \zeta_j$ is small, for some ζ_j), generate very large terms in the sum. In fact, the integrand is nearly singular, so only poor accuracy is expected. Instead, the technique of singularity subtraction (referenced in §3.2.2) uses the result from (10):

$$\frac{1}{2\pi i} \sum_{j=1}^N \frac{W(\zeta_j) - W(z)}{\zeta_j - z} w_j = 0.$$

The integrand is now smooth, and good results can be expected from quadrature. This yields $W(z)$ as a 'corrected' (19):

$$W(z) = \left[\sum_{j=1}^N \frac{W(\zeta_j)}{\zeta_j - z} w_j \right] / \left[\sum_{j=1}^N \frac{1}{\zeta_j - z} w_j \right].$$

Implementation of the CBIEM using this result is successful. The code supplied (see §4) does not go beyond the stage of the computation of $\hat{\mathbf{V}}$ on Γ , as it is known that the approximation to U in the interior is actually *more* accurate than the approximations to V on the boundary [3]. Experiment demonstrates this, and thus computation of U at interior points need not be further described.

3.4 Performance of the CBIEM on Model Problems

Application of the CBIEM yields different quality results depending on the continuity of the model problem and the contour. In the simplest case, both are smooth, there is no singularity, and standard quadrature gives good results. In fact, because of periodicity, even the trapezoidal rule on a uniform mesh gives very good results. There is no need to use h - p quadrature, but it will still work well.

Now consider the case where Γ is smooth, but W has singularities. For example, if $W(\gamma(s)) \sim s^{1/2}$, the integrand of the CBIE (9) can have behaviour $s^{-1/2}$ near the corner. However, using singularity subtraction and h - p quadrature, experiment demonstrates that both the discretisation error and the final error in $\hat{\mathbf{V}}$ on the boundary are superb. (See also the example of complex contour integration in §2.6.4.)

If W is smooth, but Γ is not (has corners), in general, the errors will be expected to increase with the sharpness of the corner. The most difficult cases are cusps or reentrant corners (e.g. the corner in a cardioid). Even for a model problem with a smooth solution U , a corner singularity in V (and hence W) will occur.

Let r represent radial distance from a corner. It is known [23, pages 257–259], that at a corner with interior angle $(1 - \chi)\pi$, a singularity of the form $r^{1/(1-\chi)}$ will be found. At worst, for a reentrant corner, $\chi = -1$, so the form is $r^{1/2}$. A good model problem is thus a contour with a corner where the true solution has local behaviour $U \sim r^{1/2}$. This is obtained, for example, using $W(z) = z^{1/2}$. If a uniform mesh were used, the greatest component of the error in V will come from the intervals adjacent to the corner. The use of a geometrically graded mesh reduces this component to a level comparable with that of other mesh intervals. Errors will not be of the very high order that is expected for smooth contours, but should still be acceptable.

3.5 Higher Degree Interpolatory Polynomials

3.5.1 Introduction

To extend the technique described in §3.2.4, the linear interpolation in (12) is replaced by a higher degree interpolation. The net result of this is to change the definition of the matrix B in (15). Other possible techniques of improving the accuracy of the interpolation, such as splines, are not considered here, as they are difficult to implement. The principle involved is that increasing the order of the interpolatory polynomial should reduce the discretisation error, which is expected to be greatest on the largest intervals.

The ‘nearest’ O node points on either side of $\zeta_{k-1/2}$ are used to yield an interpolatory polynomial of degree $O-1$. In general, for points far from the nearest corner, this means to take the first O terms of the sequence $\zeta_k, \zeta_{k-1}, \zeta_{k+1}, \zeta_{k-2}, \dots$. Otherwise, the term ‘nearest’ is used loosely, as interpolation cannot continue around a corner. Where there are less than $O/2$ node points between the collocation point and the nearest corner (including the node on the corner); instead O points from and including the corner are used. This results in an interpolatory polynomial that is expected to be least accurate at the collocation point adjacent to the corner. (A possible improvement in this schema is to organise the interpolation rules such that their order increases say, linearly, with node index away from the corner.) The constraint on O due to the mesh parameter D is described in §3.5.4.

§§3.5.2 and 3.5.3 deal with technical implementation issues, and can be skipped without loss of continuity.

3.5.2 Lagrange Form of the Interpolatory Polynomial

The Lagrange form of the interpolatory polynomial is used. Given a set of values for the V_j , at positions $\zeta_j = \gamma(t_j)$, the approximation to V at point $\zeta_{k-1/2}$ is:

$$V(\zeta_{k-1/2}) \approx \hat{V}_{k-1/2} = \sum_{j \in F_k} \lambda_j(t_{k-1/2}) V_j.$$

Here:¹⁷

$$\lambda_j(t) = \prod_{\nu \in F_k, \nu \neq j} \frac{t - t_\nu}{t_j - t_\nu}.$$

F_k is a set of indices of the nearest node points, specific to the collocation point $\zeta_{k-1/2}$. Specifically, where a degree $O-1$ interpolatory polynomial is used on O points, and C is the index of the nearest corner to $\zeta_{k-1/2}$:

$$F_k = \begin{cases} \{k - O/2, \dots, k - 1, k, \dots, k + O/2 - 1\} & \text{in general} \\ \{C, \dots, C + O - 1\} & \text{if } k - O/2 < C \\ \{C - O + 1, \dots, C\} & \text{if } k + O/2 > C. \end{cases}$$

Let F_k be the k th row of a table F , and let the above λ_j be the j th element of the k th row of another table, L , of the associated weights. The notations $F(k, j)$ and $L(k, j)$ are used to describe the set of O nodal indices and weights associated with the interpolation at point $\zeta_{k-1/2}$, where $k = 1 : N$ and $j = 1 : O$. The structure of F becomes more complicated with increasing O and with increasing number of corners. Details of its construction are not provided here, but can be read from the program `cbiem.m` in Appendix A.1.

¹⁷Warning: Replacing t_ν with ζ_ν and t_j with ζ_j in this formula *cannot* be done, as the contour segments are *not* necessarily straight.

For some integer D , on each segment of Γ (with a corner at each end), a mesh is constructed that has $D - 1$ internal points between each corner and a (wide) interval which spans the centre of the segment. This results in a total of $2D$ mesh points, and $2D - 1$ mesh intervals (see Figure 4).

For example, if $D = 3$, then there are 4 interior and 2 corner mesh points on each segment, together with 4 extra interior points, for a total of $S = (D + 1)^2 + 1 = 10$. Further, if there are $NC = 3$ corners, then the linear system has order $N = NC(S - 1) = 27$. If $O = 6$ (quintic interpolation about the ‘nearest’ 6 points), then $F \in \mathbb{N}^{N \times O}$. Where divisions in the structure of F due to the corners are reflected by partitions, F is:¹⁸

$$F = \begin{bmatrix} 27 & 1 & 2 & 3 & 4 & 5 \\ 27 & 1 & 2 & 3 & 4 & 5 \\ 27 & 1 & 2 & 3 & 4 & 5 \\ 1 & 2 & 3 & 4 & 5 & 6 \\ 2 & 3 & 4 & 5 & 6 & 7 \\ 3 & 4 & 5 & 6 & 7 & 8 \\ 4 & 5 & 6 & 7 & 8 & 9 \\ 4 & 5 & 6 & 7 & 8 & 9 \\ 4 & 5 & 6 & 7 & 8 & 9 \\ \hline 9 & 10 & 11 & 12 & 13 & 14 \\ 9 & 10 & 11 & 12 & 13 & 14 \\ 9 & 10 & 11 & 12 & 13 & 14 \\ 10 & 11 & 12 & 13 & 14 & 15 \\ 11 & 12 & 13 & 14 & 15 & 16 \\ 12 & 13 & 14 & 15 & 16 & 17 \\ 13 & 14 & 15 & 16 & 17 & 18 \\ 13 & 14 & 15 & 16 & 17 & 18 \\ 13 & 14 & 15 & 16 & 17 & 18 \\ \hline 18 & 19 & 20 & 21 & 22 & 23 \\ 18 & 19 & 20 & 21 & 22 & 23 \\ 18 & 19 & 20 & 21 & 22 & 23 \\ 19 & 20 & 21 & 22 & 23 & 24 \\ 20 & 21 & 22 & 23 & 24 & 25 \\ 21 & 22 & 23 & 24 & 25 & 26 \\ 22 & 23 & 24 & 25 & 26 & 27 \\ 22 & 23 & 24 & 25 & 26 & 27 \\ 22 & 23 & 24 & 25 & 26 & 27 \end{bmatrix} = \begin{bmatrix} Ft(1) \\ Ft(2) + S * \text{ones}(Ft) \\ \vdots \\ Ft(NC) + (NC - 1)S * \text{ones}(Ft) \end{bmatrix}.$$

For $j = 1 : S - 1$ and $k = 1 : O$, in general $Ft \in \mathbb{N}^{(S-1) \times O}$ is:

$$Ft(j, k) = \begin{bmatrix} k - 1 & j \leq O/2 \\ k - 1 + j - O/2 & O/2 < j < S - O/2 \\ k - 1 + S - O & S - O/2 \leq j \end{bmatrix}.$$

(Exception: $F(1 : O/2, 1) \Leftarrow N \times \mathbf{1}_{O/2}$.)

3.5.3 Construction of B

The matrix B is required in the construction of the linear system in (16), and is the only thing that changes when O is varied. For the case of linear interpolatory polynomials ($O = 2$), a formula involving the terms H_k is used to approximate the value of V at the collocation points. For larger O , this is replaced with a considerably more sophisticated formula. As O increases, the bandwidth of B increases. Naturally, this new B simplifies to the earlier definition if $O = 2$ is used, but is obtained at greater computational expense.

The crucial change is in the approximation to the value of $V_{k-1/2}$, which in (13) is the term $\frac{1}{2}V_{k-1} + \frac{1}{2}V_k$. This is now replaced with:

$$\sum_{j \in F_k} \lambda_j (\zeta_{k-1/2}) V_j = \sum_{j=1}^O L(k, j) V_{F(k, j)}.$$

¹⁸Liberal use of MATLAB notation is made, and there is a confusion between computer array element and mathematical matrix entry notation: $F(j, k) \equiv F_{j,k}$.

The first O terms of the LHS of the k th line of (13) (there is only one other term) are now:

$$\sum_{j=1}^O L(k, j) V_{F(k,j)} H_k.$$

Construction of the real order N matrix with (k, j) th entry $L(k, j) V_{F(k,j)}$ is required. Multiplying each row by the corresponding H_k converts this to B .

Details of the construction of B are not provided here, but the illustrative example used in §3.5.2 is continued. Recall that $D = 3$, $NC = 3$ and $O = 6$, so $S = 10$, and $N = 27$. First construct Bt (a ‘skewed’ version of L), and then calculate B by multiplying Bt through by the H_k . Bt is constructed using a ‘shift vector’ G , where G_k is equal to the number of zeros to be put in front of row k of L to make it row k of Bt . This G has a structure formed from a temporary Gt :

$$\begin{aligned} Gt &= \left[\text{zeros}(1, O/2) \quad [1 : S - O - 1] \quad (S - O) \mathbf{1}_{O/2}^\top \right]^\top \\ G &= [Gt \quad Gt + S - 1 \quad \dots \quad Gt + NC(S - 1)]^\top \\ Bt(k, :) &= [\text{zeros}(1, G(k)) \quad L(k, :) \quad \text{zeros}(1, N - G(k) - O/2)]^\top \quad k = 1 : N \\ B &\Leftarrow Bt(:, 2 : N) \quad B(1 : O/2, N) \Leftarrow Bt(1 : O/2, 1). \end{aligned}$$

The overall structure of B is depicted in Figure 5, where \times and \cdot represent nonzero and zero entries respectively.



Figure 5: Structure of B .

The $NC \times NC$ submatrices within the structure are each of order $S - 1$. The k th row generally consists of $O = 6$ contiguous nonzero entries, starting at column G_k . These entries are the k th row of L , multiplied by H_k . That is, the string of $O = 6$ nonzero elements in row k represents:

$$[H_k L_{k,1} \quad H_k L_{k,2} \quad \dots \quad H_k L_{k,O-1} \quad H_k L_{k,O}].$$

Additionally, in the first $O/2$ rows, the first of these O entries is shifted to the N th column, due to a ‘wraparound’ effect. In view of the banded structure of B , it appears that a method designed to exploit this structure would be appropriate in the solution of (18). Unfortunately A is neither banded, nor of a particularly simple structure, so this approach is nontrivial, and is a direction for further work.

3.5.4 Limitations on the Degree of the Interpolatory Polynomial

The discussion and results presented in §2 prompt the use of a geometrically graded mesh, with the number of points in the (closed) quadrature rule on each mesh interval linearly increasing with interval number from the corner, beginning with 2 adjacent to the corner, and becoming D on the central (widest) interval. The use of a linear grading is found in the literature of the finite element method and the usual boundary element method [1, 19]. Changing from linear to quadratic or higher degree may reduce the errors, but its implementation is beyond the scope of this report.

Consider a segment of Γ divided into a mesh on $2(D+1)$ points, including corners, with $m = 2D+1$ intervals. Basic quadrature rules on $n_j = 2, 3, \dots, D-1, D, D-1, \dots, 3, 2$ points, are used over intervals $j = 1 : m$. After all of the common end points are considered, the total number of points in the final composite quadrature rule for that segment is $S = (D+1)^2 + 1$. Slightly different results would apply if the quadrature rules were open. Recall that this choice is rejected, as it leads to node points that avoid the singularity.

S imposes a limit on O , the number of points used in the interpolation rule. As O is usually small (for reasons of computational efficiency, typically $O \leq 6$), this limitation is usually not significant. For example, if $D = 2$, $O \leq 8$, and if $D = 3$, $O \leq 16$.

4 Implementation and Results

4.1 Implementation

The CBIEM is implemented as a set of functions in MATLAB¹⁹ code, presented in Appendix A. (These functions appear in alphabetic order, interspersed with several functions referenced in §2.) The main routine is `cbiem.m`. The parameterisation of the contour and its derivative are computed within `cbiem.m`, and it calls an auxiliary function (`funcCb.m`) to compute the true solution for a test problem. The quadrature points for basic rules are obtained by calling the function `gettw.m`, which provides either (closed) Newton–Cotes points (using a routine internal to `gettw.m`), or calls another function, `lobatto.m`, which computes the points for a closed Gauß–Lobatto rule. Two further functions are used to create an h - p composite quadrature rule out of a set of basic quadrature rules (`hprmesh.m`), and compose a quadrature rule over a contour with several corners (`rsmesh.m`). For testing `cbiem.m` over a large set of parameters (e.g. generating the data for Tables 2 to 10), a driver function, `testcb.m`, is used.

Within `cbiem.m` is a description of its input parameters. For test problems, where the true solution is known, it plots and calculates norms of $\mathbf{V} - \hat{\mathbf{V}}$, and also calculates some discretisation errors. Explicit computation of the approximate solution within Ω is *not* performed. Experiments with doing this demonstrate that the error results obtained are of the same order as those returned.

¹⁹MATLAB is an (interpreted) matrix computation package, and is a trademark of The Mathworks, Inc.

4.2 Experimental Results using a Teardrop Contour

4.2.1 Description

Although the CBIEM code is generalised to the situation of multiple corners, good experimental contours have only one corner, to facilitate isolation of the sources of error. This section describes numerical results for the CBIEM, using a teardrop contour,²⁰ depicted in Figure 6. The contour is parametrically given by:

$$\gamma(t) = 2 \sin(\pi t) + i \sin(2\pi t) \quad t \in [0, 1].$$

This is the same contour as that used in [3]. It has a right angle corner at the origin, which facilitates the use of test problems $W(z) = z^\alpha$. For $\alpha \in (0, 1)$, there is a discontinuity in the derivative of the true solution at the origin, which becomes more pathological as $\alpha \rightarrow 0$.

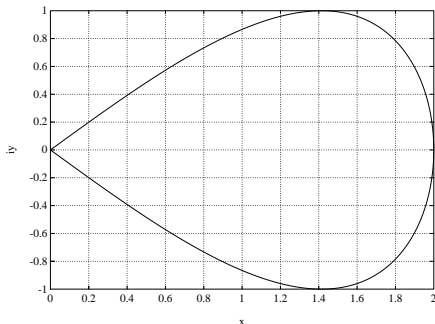


Figure 6: Teardrop contour used in the CBIEM experiments.

Error results are presented using an unweighted vector 2 norm:

$$\|\mathbf{V} - \hat{\mathbf{V}}\|_2 = \left[\sum_{i=1}^N (V_i - \hat{V}_i)^2 \right]^{1/2}.$$

An appropriately weighted discretisation of the L_2 norm might seem more appropriate, but would effectively only present the norm over the central interval, as the widths of the end point intervals are very small. The use of an infinity norm is also appealing, but the 2 norm allows the user to experiment with interpolation formula gradings, to independently reduce the error over different regions of the contour (see §4.2.6). Also, experimental data shows the behaviour of the infinity norm is very similar to that of the 2 norm.

Tables 2 to 10 present error results for the teardrop contour, for three different model problems: $W(z) = z^2$, $z^{1/2}$ and $z^{1/4}$; various choices of two mesh grading parameters (σ and D); and choices of O , the number of points used by the interpolatory polynomial in the collocation process. In each table $N = (D + 1)^2$ is the size of the linear system being solved, such that there are $2D + 1$ mesh intervals between one corner and the next (see §3.5.2). The nine tables cover three illustrative choices of the mesh parameter σ for each of the three model problems. In each case, the results presented are for a choice of σ close to the optimal σ , and two nearby values of σ that demonstrate the increase in the error in each direction. Results have been selected from a much larger data set. Within each table, the minimum error result is emboldened.

²⁰Another important test contour is a cardioid with a reentrant corner.

4.2.2 Observations of z^2

This test function does *not* have a singularity, and the results are good. Despite the corner, the error reduces with increasing either D or O , until a point is reached where roundoff error, caused by excessive order in the interpolatory polynomial, begins to encroach.

	O							
N	8	10	12	14	16	18	20	22
25	4.6e-04	5.6e-05	6.0e-06	1.0e-06	1.2e-06	1.2e-06	3.7e-06	3.0e-06
36	1.4e-04	1.3e-05	1.1e-06	8.0e-08	4.2e-08	2.8e-08	7.8e-07	4.1e-07
49	7.1e-05	5.7e-06	3.9e-07	2.5e-08	5.6e-09	3.5e-10	5.8e-08	2.9e-05
64	3.1e-05	2.1e-06	1.2e-07	6.5e-09	1.5e-09	9.0e-09	2.6e-07	5.2e-02
81	1.6e-05	1.0e-06	5.5e-08	2.5e-09	3.6e-10	1.2e-08	3.6e-05	2.0e-02
100	8.6e-06	4.9e-07	2.3e-08	9.6e-10	8.4e-10	1.0e-08	4.2e-05	1.6e-01

Table 2: $\sigma = 0.20$, $U(z) = \Re(z^2)$.

	O							
N	8	10	12	14	16	18	20	22
25	5.9e-05	6.6e-06	9.0e-06	9.3e-06	9.3e-06	9.4e-06	9.3e-06	9.7e-06
36	1.5e-05	9.3e-07	1.8e-07	2.2e-07	2.3e-07	2.3e-07	2.4e-07	1.4e-06
49	6.2e-06	3.1e-07	1.2e-08	5.0e-09	5.5e-09	5.5e-09	6.9e-09	6.7e-08
64	2.6e-06	1.0e-07	4.0e-09	9.9e-11	1.2e-10	1.3e-10	1.5e-10	4.7e-09
81	1.3e-06	4.5e-08	1.4e-09	4.1e-11	2.3e-12	3.1e-12	4.6e-12	8.1e-09
100	6.7e-07	2.0e-08	5.7e-10	1.4e-11	3.8e-13	5.2e-13	2.5e-11	4.6e-08

Table 3: $\sigma = 0.28$, $U(z) = \Re(z^2)$.

	O							
N	8	10	12	14	16	18	20	22
25	1.3e-04	1.4e-04	1.4e-04	1.4e-04	1.4e-04	1.4e-04	1.4e-04	1.4e-04
36	6.3e-06	6.7e-06	6.8e-06	6.8e-06	6.8e-06	6.8e-06	6.8e-06	6.8e-06
49	3.4e-07	3.1e-07	3.2e-07	3.2e-07	3.2e-07	3.2e-07	3.2e-07	3.2e-07
64	1.1e-07	1.3e-08	1.5e-08	1.5e-08	1.5e-08	1.5e-08	1.5e-08	1.5e-08
81	5.4e-08	7.9e-10	6.8e-10	6.9e-10	6.9e-10	6.9e-10	6.9e-10	6.9e-10
100	2.6e-08	3.7e-10	2.8e-11	3.1e-11	3.1e-11	3.1e-11	3.1e-11	3.1e-11

Table 4: $\sigma = 0.35$, $U(z) = \Re(z^2)$.

4.2.3 Observations of $z^{1/2}$

This case has a corner singularity, and represents the ‘worst’ that singularities get in practice (that is, for z^α singularities, in practice $\alpha \geq 1/2$). Although the error decreases with increasing D or O , it does so more slowly than for z^2 , and is orders of magnitude larger. As for z^2 , there comes a point where increasing O causes the error to increase, and indeed grow exponentially. The results for $\mathbf{V} - \hat{\mathbf{V}}$ for the case $\sigma = 0.10$, $D = 9$, $O = 6$ are plotted in Figure 7. The abscissae are plotted uniformly, for if they were plotted versus parameter t , the geometric grading would bunch up most of the results at the ends (corner of teardrop). Observe that these results are, as expected, antisymmetric.

	O				
N	2	4	6	8	10
16	2.2e-02	1.1e-02	2.6e-02	7.3e-01	2.3e+00
25	1.4e-02	6.6e-03	8.5e-03	1.8e-01	4.5e+00
36	1.0e-02	2.2e-03	2.1e-03	4.3e-02	5.3e+00
49	8.1e-03	1.3e-03	9.3e-04	9.7e-03	1.8e+00
64	6.3e-03	6.8e-04	3.6e-04	2.2e-03	4.5e-01
81	4.9e-03	4.5e-04	1.9e-04	5.5e-04	1.0e-01
100	3.9e-03	2.9e-04	1.1e-04	1.7e-04	2.2e-02

Table 5: $\sigma = 0.05$, $U(z) = \Re(z^{1/2})$.

	O				
N	2	4	6	8	10
16	2.0e-02	1.4e-02	1.3e-02	4.4e-02	2.7e-01
25	1.2e-02	5.2e-03	5.1e-03	1.4e-02	1.4e-01
36	8.3e-03	1.6e-03	1.5e-03	4.5e-03	4.9e-02
49	5.9e-03	6.2e-04	5.2e-04	1.4e-03	1.5e-02
64	4.5e-03	2.5e-04	1.6e-04	4.5e-04	4.9e-03
81	3.4e-03	1.3e-04	6.0e-05	1.4e-04	1.5e-03
100	2.7e-03	8.4e-05	2.4e-05	4.6e-05	4.9e-04

Table 6: $\sigma = 0.10$, $U(z) = \Re(z^{1/2})$.

	O				
N	2	4	6	8	10
16	2.4e-02	2.3e-02	2.2e-02	2.8e-02	3.0e-02
25	1.2e-02	9.7e-03	9.3e-03	1.1e-02	1.3e-02
36	7.0e-03	3.7e-03	3.5e-03	4.3e-03	5.4e-03
49	4.7e-03	1.4e-03	1.3e-03	1.6e-03	2.1e-03
64	3.4e-03	5.7e-04	5.3e-04	6.5e-04	8.2e-04
81	2.6e-03	2.3e-04	2.0e-04	2.5e-04	3.1e-04
100	2.0e-03	9.8e-05	8.0e-05	9.8e-05	1.2e-04

Table 7: $\sigma = 0.15$, $U(z) = \Re(z^{1/2})$.

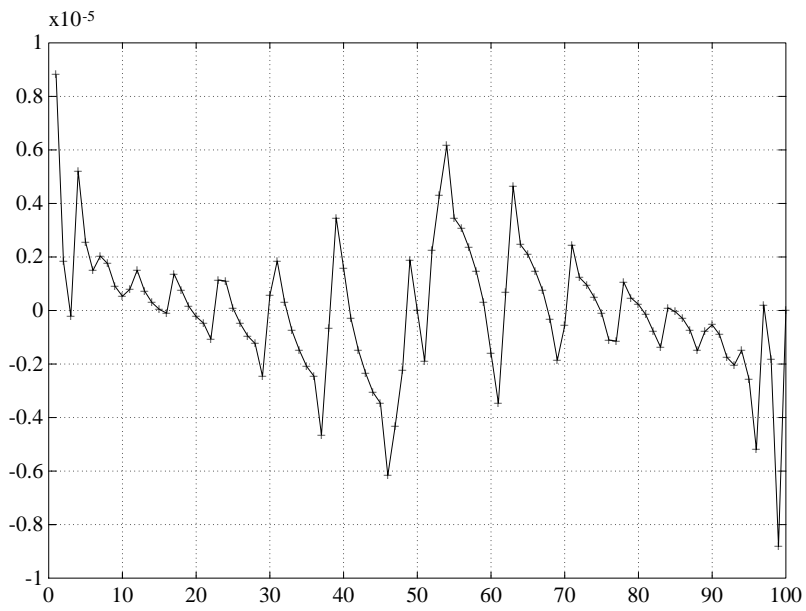


Figure 7: $\mathbf{V} - \hat{\mathbf{V}}$ for Table 6, using $D = 9$, $O = 6$.

4.2.4 Observations of $z^{1/4}$

A $z^{1/4}$ singularity is beyond the range of singularities expected for smooth test functions. The errors are worse again than for $z^{1/2}$, and they do not decrease as fast with increasing D or O . In fact, when the test problem is this pathological, the Dirichlet problem is fast becoming a boundary layer problem, which should be dealt with using more specialised methods.

	O			
N	2	4	6	8
16	4.6e-02	4.4e-02	8.1e-01	1.0e+01
25	3.2e-02	3.3e-02	2.8e-01	3.2e+01
36	1.7e-02	1.9e-02	1.0e-01	4.9e+01
49	1.0e-02	1.2e-02	4.1e-02	3.3e+01
64	5.9e-03	6.9e-03	1.6e-02	1.3e+01
81	3.9e-03	4.2e-03	7.5e-03	1.8e+01
100	2.9e-03	2.5e-03	3.6e-02	2.8e+02

Table 8: $\sigma = 0.02$, $U(z) = \Re(z^{1/4})$.

	O			
N	2	4	6	8
16	3.6e-02	3.8e-02	5.8e-02	1.4e+00
25	2.0e-02	2.1e-02	3.0e-02	7.5e-01
36	1.0e-02	9.8e-03	1.4e-02	3.6e-01
49	5.4e-03	4.9e-03	7.1e-03	1.7e-01
64	3.2e-03	2.3e-03	3.3e-03	8.3e-02
81	2.1e-03	1.1e-03	1.6e-03	4.0e-02
100	1.6e-03	5.6e-04	7.8e-04	2.0e-02

Table 9: $\sigma = 0.05$, $U(z) = \Re(z^{1/4})$.

	O			
N	2	4	6	8
16	5.8e-02	6.0e-02	5.8e-02	6.4e-02
25	3.4e-02	3.5e-02	3.4e-02	3.7e-02
36	1.9e-02	1.9e-02	1.9e-02	2.0e-02
49	1.1e-02	1.1e-02	1.0e-02	1.1e-02
64	6.2e-03	6.2e-03	6.0e-03	6.5e-03
81	3.6e-03	3.5e-03	3.3e-03	3.7e-03
100	2.1e-03	1.9e-03	1.8e-03	2.0e-03

Table 10: $\sigma = 0.10$, $U(z) = \Re(z^{1/4})$.

4.2.5 The Black Art of Choosing σ

The minimum error results obtained for each test problem are plotted versus σ in Figure 8, and demonstrate that there is an optimal choice of σ , which varies significantly with the test problem. The use of the CBIEM in applications, where the true solution is not known in advance, could falter on the setting of σ . If the computational cost is to be minimised, then it is important to find the optimal σ , however, it may be expensive to try many σ until the optimal one is found. The literature does not justify a choice of σ , but merely states it, e.g. [22] uses $\sigma = 0.15$ for a particular (finite element) application. The optimal choice of σ for the paradigm test problem $z^{1/2}$ is $\sigma = 0.10$. As $z^{1/2}$ is the worst singularity expected in practice (see §3.4), this should be a good guide as a starting guess for any problem with an unknown solution.

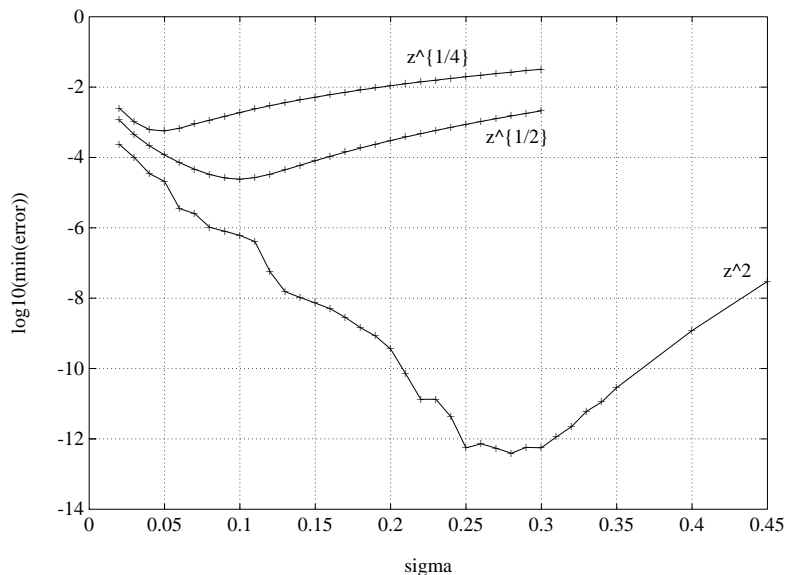


Figure 8: Variation of minimum error with σ .

4.2.6 Improvements in the Technique

Consider Table 6, where the best error result is obtained using $O = 6$. The error may be able to be reduced by grading the order of the interpolatory polynomial over the mesh intervals. Near the corner, the use of high order interpolation may actually *increase* the component of the error, although this may be appropriate far away from the corner. It may be ideal to grade the order of the interpolatory polynomial from $O = 2$ near the corner, to $O = 6$ (or greater) farthest from the corner.

Direct implementation of this result requires extensive modification to the matrix B used by the CBIEM²¹ (see §3.5.1), and is beyond the scope of this report. Another way of achieving the same effect is to calculate B matrices B_2, B_4, \dots, B_{16} for $O = 2, 4, \dots, 16$, then construct a new B from appropriate rows of them, and insert this new B at the relevant point in the CBIEM.

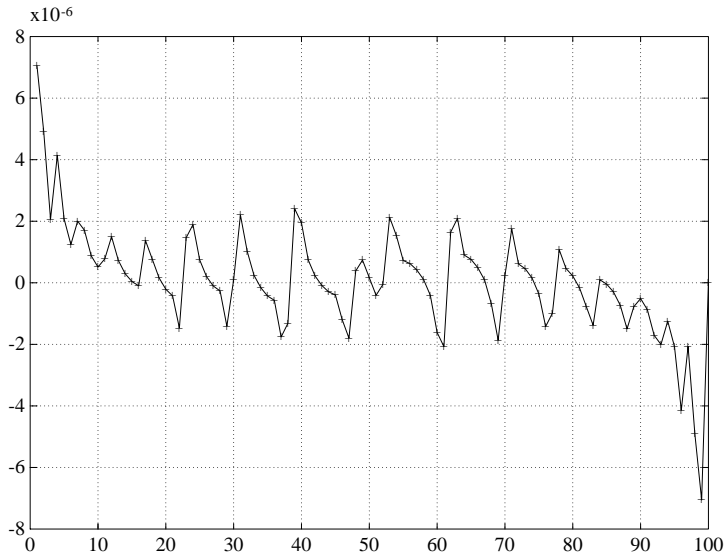


Figure 9: The best error results for $z^{1/2}$, $D = 9$, $\sigma = 0.10$ and a graded interpolation rule. c.f. Figure 7.

However, intuition is misleading here. The minimum error in Table 6 is 2.4158×10^{-5} , using $\sigma = 0.10$ and $D = 9$. This corresponds to $O = 6$ on each mesh interval. Many experiments in variation of the order of the interpolation rule, holding fixed σ and D , find that the very best error result that can be obtained is 1.7444×10^{-5} (a 28% reduction), using a grading with interpolation rules of $O = 12, 2, 2, 6, 6, 6, 10, 10, 10$ over the 9 mesh intervals from the corner to the centre. Surprisingly, the component of the error over the first interval *decreases* with increasing O . This is depicted in Figure 9, which shows that the error is uniformly distributed around the contour, except for the largest component, at the corner.

It appears that what is happening is that the method has come up against a discretisation error barrier. For this problem, the discretisation error does not decrease particularly quickly, and is a maximum at the corner.

²¹These comments also refer to the associated F and L matrices.

5 Further Directions for Research

This section enumerates various possibilities for future work on the CBIEM.

1. There is the potential for error reduction using graded interpolation rules (see §4.2.6). Similarly, other choices for the grading of the quadrature rules may assist in error reduction, e.g. quadratic increase in degree of quadrature rule with node number from the corner, rather than linear as is presently used.
2. A proper examination of the computational efficiency of the CBIEM is required. This would involve setting up, say, a finite difference solution for the Dirichlet problem, and comparing flop counts required to obtain comparable accuracies.
3. Analysis of the choice of optimal σ is desirable. Currently, the method is hampered by this not being known in advance.
4. Application of the technique to conformal mapping [7] may be worthwhile.
5. It would be computationally efficient if solution of the linear system involving the matrix $C = B - A$ could exploit the banded structure of B (see §3.5.3).
6. An alternative collocation technique is possible [20]. Given nodes ζ_j with weights w_j , and collocation points $\zeta_{j+1/2}$ with weights $w_{j+1/2}$:

$$\oint_{\Gamma} F(\zeta) d\zeta \approx \sum_{j=1}^N F(\zeta_j) w_j \approx \sum_{k=1}^N F(\zeta_{k-1/2}) w_{k-1/2}.$$

Approximate the unknowns $V_j = V(\zeta_j)$ by collocating at $\zeta_{k-1/2}$, and the unknowns $V_{k-1/2} = V(\zeta_{k-1/2})$ by collocating at ζ_j . This gives an order $2N$ system for the $2N$ unknowns V_j and $V_{k-1/2}$, but avoids interpolation.

$$\begin{aligned} 0 &= \sum_{j=1}^N \frac{W_j - W_{k-1/2}}{\zeta_j - \zeta_{k-1/2}} w_j \\ 0 &= \sum_{k=1}^N \frac{W_{k-1/2} - W_j}{\zeta_{k-1/2} - \zeta_j} w_{k-1/2}. \end{aligned}$$

The technique appears to be computationally wasteful, but may be worth investigating, as it would be simpler to implement.

7. The CVBEM was developed to solve 2D fluid flow problems [15],²² where components of the complex potential (the fluid potential Φ or the streamline function Ψ) are known at different points around the contour, typically from physical measurements.²³ A modification of the CBIEM can convert it to become a solver for Neumann (and thence mixed) boundary value problems. In the Neumann boundary value problem, U_ν , the derivative of U across Γ , is known instead of U . Use the Cauchy–Riemann equations to observe that $U_\nu = \pm V_\tau$ (the tangential component of V). The boundary information can be used to construct an approximation to V , by integration of V_τ around Γ , using a suitable zero point (adding in a constant):

$$V(\gamma(t)) = \int_0^t V_\tau(\gamma(t')) dt'.$$

The same collocation process previously used to approximate V can in this case be used to approximate U .

Beyond this, the technique is particularly applicable to free boundary problems [8], and may be able to be generalised to other elliptic (and possibly other second order) operators.

8. The method would easily parallelise. The establishment of the linear system is computationally expensive, more so for high order interpolatory polynomials. This, as well as solution of the linear system, would efficiently (geometrically) parallelise.

²²Other references to the CVBEM include [10, 16, 17, 21].

²³Warning: the notation used here $W = U + iV$ is equivalent to the fluid flow notation $W = \Phi + i\Psi$, so that U and V here have a different meaning from the fluid flow case, where they are commonly the components of the velocity $q = U\hat{\mathbf{i}} + V\hat{\mathbf{j}}$, and $U = \frac{\partial\Phi}{\partial x} = \frac{\partial\Psi}{\partial y}$, $V = \frac{\partial\Phi}{\partial y} = -\frac{\partial\Psi}{\partial x}$.

A Listing of matlab “.m” files

A.1 cbiem.m

```
function Vnorm = cbiem(CCCase, D, sigma, O, alpha);

%function Vnorm = cbiem(CCCase, D, sigma, O, alpha);
%
%       Perform the CBIEM on the Dirichlet problem.
%
%       David De Wit   March 30 1992 - January 14 1993

%%%%%%%%%%%%%%%%%%%%%%%%%%%%%%%%%%%%%%%%%%%%%%%%%%%%%%%%%%%%%%%%%%%%%%%%

% 0.0:  Input and other parameters, together with definitions.

if ~exist('alpha'), alpha = 2/3; end
if ~exist('O'),      O = 12;      end
if ~exist('sigma'), sigma = 0.32; end
if ~exist('D'),      D = 7;       end
if ~exist('CCCase'), CCCase = 4;  end

format short e;                               format compact;

%%%%%%%%%%%%%%%%%%%%%%%%%%%%%%%%%%%%%%%%%%%%%%%%%%%%%%%%%%%%%%%%%%%%%%%%
%
% CCCase:Index number to the contour being used:
%       1: Unit circle, with 4 equally spaced artificial corners.
%       2: Chandler's Teardrop, one corner, right angled, at the origin.
%           (This has been reversed to make it ACW. Now different
%           from both GAC and DDW thesis.)
%       3: Kress' ACW Teardrop, one corner, 2 pi/3 - angled.
%       4: Kress' Reentrant contour, 3 pi/2 - angled. Reversed to
%           avoid the branch cut on the negative real axis, and
%           make it ACW in orientation.
%       5: ACW Cardioid. Reentrant contour with 2 pi interior angle.
%       6: ACW Heart. Reentrant contour with 2 pi and 0 interior angles.
%       7: ACW Controlled Cardioid, using trig parameterisation.
%       8: ACW Controlled Cardioid, using polynomial parameterisation.
%       9: Modified Boomerang, with a 5 degree external angle.
%
% D:     Density of the geometric mesh, a positive integer. Choice
%       of D forces N, the size of the linear system being solved,
%       to be  $N = NC \cdot (D+1)^2$ .
%
% sigma: Mesh parameter. Ratio of distances of consecutive mesh points
%       from the nearest corner.  $0 < \sigma < 0.5$ . Try  $\sigma = 0.25$ 
%       as a starting guess.
%
% O:     Order of the interpolatory polynomial used to approximate
%       V at the collocation points. Actually the (even) number of
%       nearest points used, thus 2 is linear, 4 is cubic. Must be
%       kept  $2 \leq O \leq NS+1$ ; in practice keep  $0 \leq O \leq 20$ . This limits
%        $O \leq 8$  for  $D = 2$ ,  $16$  for  $D = 3$ , etc.
%
% alpha: Exponent of the true solution of test problem,  $W = z^{\alpha}$ .
%
% NC:    Numbers of corners/segments of the contour.
%
% NS:    Number of points on each side of the contour. N node points
%       create  $NS = (N+1)^2 + 1$  mesh points on each segment.
%%%%%%%%%%%%%%%%%%%%%%%%%%%%%%%%%%%%%%%%%%%%%%%%%%%%%%%%%%%%%%%%%%%%%%%%
```

```

% 1.1: Generate quadrature rule for a geometrically graded mesh, on
%      one segment in the t domain using hprmesh, then insert this
%      into the grid with corners, using rmesh.

numcorn = [4 1 1 1 1 1 1 1 1 1];      NC = numcorn(CCcase);

% graded mesh
G = [0 sigma.^(D:-1:1)]';             G = [G; 1-G(D+1:-1:1)];
S = [2:D+2, D+1:-1:2]';              c = [0:NC]'/NC;
[t, w] = hprmesh(G, S, 0);           [tn, wn] = rmesh(c, t, w, 1);
N = length(tn);

% Uniform mesh
%%% N = (D+1)^2;      tn = [1:N]'/N;  wn = ones(size(tn))/N;

%%%%%%%%%%%%%%%%%%%%%%%%%%%%%%%%%%%%%%%%%%%%%%%%%%%%%%%%%%%%%%%%%%%%%%%%

% 1.2: Compute the (complex) values of zn and zc (z at the node and
%      collocation points specified by tn and tc, respectively).
%      zc are found as the midpoints of zn in an arc-length sense, by
%      mapping the midpoints of tc to the contour. Also calculate
%      gdot, which is used to modify wn.

tc = tn - diff([0; tn])/2;
ptn = pi*tn;                          ptc = pi*tc;
if (CCcase == 1)
    zn = exp(2*i*ptn);                 zc = exp(2*i*ptc);
    gdot = 2*pi*i*exp(2*i*ptn);
elseif (CCcase == 2) % Chandler's Teardrop
    zn = 2*sin(ptn) - i*sin(2*ptn);
    zc = 2*sin(ptc) - i*sin(2*ptc);
    gdot = 2*pi*(cos(ptn) - i*cos(2*ptn));
    gdot(N) = -2*pi*i;
elseif (CCcase == 3) % Kress's Teardrop
    zn = sin(ptn)*2/sqrt(3) - i * sin(2*ptn);
    zc = sin(ptc)*2/sqrt(3) - i * sin(2*ptc);
    gdot = 2*pi*( cos(ptn)/sqrt(3) - i*cos(2*ptn) );
    gdot(N) = -2*pi*i;
elseif (CCcase == 4) % Kress's Boomerang
    a = 2/3;
    zn = - a * sin(3*ptn) - i * sin(2*ptn);
    zc = - a * sin(3*ptc) - i * sin(2*ptc);
    gdot = - 2*pi*( (3*a/2)*cos(3*ptn) + i*cos(2*ptn) );
    gdot(N) = -2*pi*i;
elseif (CCcase == 5) % Plain Cardioid
    zn = (-1 + cos(2*ptn)).*exp(i*2*ptn);
    zc = (-1 + cos(2*ptc)).*exp(i*2*ptc);
    gdot = -2*pi*exp(i*2*ptn).*(sin(2*ptn) + i*(1-cos(2*ptn)));
    gdot(N) = 0;
elseif (CCcase == 6) % Pointed Heart - Silly
    zn = - sin(3*ptn) - i*(sin(2*ptn)).^3;
    zc = - sin(3*ptc) - i*(sin(2*ptc)).^3;
    gdot = - 3*pi*( cos(3*ptn) + i*2*cos(2*ptn).*(sin(2*ptn)).^2 );
    gdot(N/2) = 0;                          gdot(N) = 0;
elseif (CCcase == 7) % My Cardioid
    zn = - sin(3*ptn) - 5 * i* tn .* (1 - tn) .* sin(2*ptn);
    zc = - sin(3*ptc) - 5 * i* tc .* (1 - tc) .* sin(2*ptc);
    gdot = - 3 * pi * cos(3*ptn) - 5 * i * ...
        ( (1-2*tn).*sin(2*ptn) + 2*ptn.*(1-tn).*cos(2*ptn) );
    gdot(N) = 0;

```

```

elseif (CCase == 8) % My Stupid Polynomial Cardioid
    a = 7/24;
    zn = tn .* (tn - a) .* (tn - 1 + a) .* (tn - 1) + ...
        i * tn.^2 .* (tn - 1/2) .* (tn - 1).^2;
    zc = tc .* (tc - a) .* (tc - 1 + a) .* (tc - 1) + ...
        i * tc.^2 .* (tc - 1/2) .* (tc - 1).^2;
    gdot = (tn - a) .* (tn - 1 + a) .* (tn - 1) + ...
        tn .* (tn-1+a) .* (tn-1) + tn .* (tn-a) .* (tn-1) + ...
        tn .* (tn-a) .* (tn-1+a) + ...
        i * ( 2 * tn .* (tn - 1/2) .* (tn - 1).^2 + ...
        2 * tn.^2 .* (tn - 1/2) .* (tn - 1) + ...
        tn.^2 .* (tn - 1).^2 );
    gdot(N) = 0;
    zn = 100*zn;    zc = 100*zc;    gdot = 100*gdot;
elseif (CCase == 9) % 5 degree external angle.
    deg = 5;
    a = 2/( 3 * tan(deg*pi/360));
    zn = - a * sin(3*pntn) - i * sin(2*pntn);
    zc = - a * sin(3*ptc) - i * sin(2*ptc);
    gdot = - 2*pi*( (3*a/2)*cos(3*pntn) + i*cos(2*pntn) );
    gdot(N) = -2*pi*i;
elseif (CCase == 10) % 20 degree external angle.
    deg = 20;
    a = 2/( 3 * tan(deg*pi/360));
    zn = - a * sin(3*pntn) - i * sin(2*pntn);
    zc = - a * sin(3*ptc) - i * sin(2*ptc);
    gdot = - 2*pi*( (3*a/2)*cos(3*pntn) + i*cos(2*pntn) );
    gdot(N) = -2*pi*i;
end

%rzn = real(zn);                izn = imag(zn);
%plot(rzn,izn,'-',rzn,izn,'+');    grid;

%plot(tn(1:10),izn(1:10),'-',tn(1:10),izn(1:10),'+');    grid;

wn = wn.*gdot;

%%%%%%%%%%%%%%%%%%%%%%%%%%%%%%%%%%%%%%%%%%%%%%%%%%%%%%%%%%%%%%%%%%%%%%%%

% 2.1: Set up the complex order N matrices A and B. Establish F, a
%       matrix of indices to be used in calculating B, using Ft, a
%       submatrix of the pattern of indices for one edge. Also compute
%       L, the matrix of the coefficients of the interpolatory
%       polynomial, using the indices contained in F.

oN = ones(N,1);                j = 0/2;
A = oN*wn.' ./ ( oN*zn.' - zc*oN');    NS = N/NC;

Ft = zeros(NS, 0);            Ft(1,:) = 0:0-1;
Ft(NS,:) = NS-0+1:NS;
Ft(2:j,:) = ones(j-1,1)*Ft(1,:);
Ft(NS-j+1:NS-1,:) = ones(j-1,1)*Ft(NS,:);
for k = j+1:NS-j, Ft(k,:) = Ft(k-1,:) + 1; end
for k = 1:NC, F((k-1)*NS+1:k*NS,:) = Ft + (k-1)*NS; end
F(1:j,1) = N*ones(j,1);

```

```

L = ones(size(F));
for k = 1:0, for v = 1:0
    if (v ~= k)
        tk = tn(F(o2,k));
        L(o2, k) = L(o2, k).*( tc(o2) - tv ) ./ ( tk - tv);
        tk = tn(F(1:j,k));
        L(o1, k) = L(o1, k) .* ( tc(o1) - tv ) ./ ( tk - tv );
    end
end, end

%%%%%%%%%%%%%%%%%%%%%%%%%%%%%%%%%%%%%%%%%%%%%%%%%%%%%%%%%%%%%%%%%%%%%%%%

% 2.2: Compute the matrix B. J is a shift vector, used to create rows
% of B from rows of L. Multiply the temporary result through by
% H, then write out C.

H = sum(A. ');
t2 = [-t1; [0:NS-0-1]'; (NS-0)*t1];
for k = 1:NC, J((k-1)*NS+1:k*NS) = t2 + (k-1)*NS; end
B(1:j,1:0-1) = L(1:j,2:0);
for k = j+1:N, B(k,J(k)+1:J(k)+0) = L(k,:); end
C = B.*(H'*ones(size(H))) - A;

%%%%%%%%%%%%%%%%%%%%%%%%%%%%%%%%%%%%%%%%%%%%%%%%%%%%%%%%%%%%%%%%%%%%%%%%

% 2.3: Set up and solve for Vn (computed approximation to V at the
% node points), the linear system:
% C Vn = A * Utn - sum(A).*Uc
% Given C, establish the real, order N-1 matrix, Cstar, then
% calculate Vn, using Vn(N) = 0.

% sprintf('Solving the linear system of size %g', N)
Un = real(funcCb(zn, alpha));
d = diag(H)*Uc - A*Un;
C = real(C(2:N,1:N-1) - C(1:N-1,1:N-1));
Vn = zeros(size(Un));

%%%%%%%%%%%%%%%%%%%%%%%%%%%%%%%%%%%%%%%%%%%%%%%%%%%%%%%%%%%%%%%%%%%%%%%%

% 2.4: Error norms. Vne and Vce are the differences between the true
% and the computed values of V at the node and collocation points
% respectively. r is the discretisation error in the CBIE. p is
% the residual in the (above) computation for Vtn, when the true
% soln at the node points is substituted into the equations.

Vne = imag(funcCb(zn, alpha)) - Vn;
Vnorm = sqrt(abs(wn)'*(Vne.^2));

% Compute the approximation at the 4 points of Kress:

Wn = Un + i * Vn;
z1 = [ 0.1+0*i 0.2+0*i 0.3+0*i 0+0.2*i ];
for j = 1:4
    WK(j) = sum(Wn .* wn ./ (zn - z1(j))) / sum(wn./(zn - z1(j)));
end
WKt = funcCb(z1, alpha);
Ek = [N 0 abs(real(WK - WKt))]

```

A.2 cint.m

```

function [rho, C] = cint(sigma);

% function [rho, C] = cint(sigma);
%
%   Contour integration with a geometric h-p grid.
%
%   David De Wit   July 14 1992 - July 17 1992

%%%%%%%%%%%%%%%%%%%%%%%%%%%%%%%%%%%%%%%%%%%%%%%%%%%%%%%%%%%%%%%%%%%%%%%%

if ~exist('QCase'), QCase = 2;   end
if ~exist('sigma'), sigma = 0.15; end

DMin = 8;                               DMax = 15;
format short e;                           format compact;
QCase = 2;

for D = DMin:DMax
    G = [0 sigma.^(D:-1:1)]';           G = [G; 1-G(D+1:-1:1)];
    S = [2:D+2, D+1:-1:2]';           NC = 2;
    [t, w] = hprmesh(G, S, QCase, 0);   c = [0:NC]'/NC;
    [tn, wn] = rmesh(c, t, w, 1);       zn = exp(2*pi*i*tn);
    iN(D-DMin+1) = length(zn);          wn = wn.*gdot;
    gdot = 2*pi*i*zn;                  ier(D-DMin+1) = 1-wn.*(((zn-1)/i).^(1/2)./zn)/(2*pi*i*sqrt(i));
end
lier = log10(abs(ier))';                sqiN = sqrt(iN)';

plot(sqiN,lier,'-g',sqiN,lier,'+r');    grid;
title('Contour integration on a h-p geometric grid');
xlabel('sqrt(N)');                       ylabel('log10(Error)');

```

A.3 funccb.m

```
function W = funccb(z, alpha);

% function W = funccb(z, alpha);
%
%       True solution to the Dirichlet problem solved by cbiem.
%
%   David De Wit   April 13 1992 - September 27 1992

%%%%%%%%%%%%%%%%%%%%%%%%%%%%%%%%%%%%%%%%%%%%%%%%%%%%%%%%%%%%%%%%%%%%%%%%

W = z.^(alpha);
```

A.4 funcci.m

```
function W = funcci(z);

% function W = funcci(z);
%
%       Integrand of the problem solved by cint.
%
%   David De Wit   July 9 1992 - July 17 1992

%%%%%%%%%%%%%%%%%%%%%%%%%%%%%%%%%%%%%%%%%%%%%%%%%%%%%%%%%%%%%%%%%%%%%%%%

W = ((z-1)/i).^(1/2)./z;
```

A.5 func hp.m

```
function f = func hp(x)

% function f = func hp(x);
%
%       Function being integrated by hpmeth.
%
%   David De Wit   July 9 1992 - July 17 1992

%%%%%%%%%%%%%%%%%%%%%%%%%%%%%%%%%%%%%%%%%%%%%%%%%%%%%%%%%%%%%%%%%%%%%%%%

f = 1 - 3/2*sqrt(x);
```

A.6 gettw.m

```

function [QRt, QRw] = gettw(R, QCase);

% function [QRt, QRw] = gettw(R, QCase);
%
%      Get tables of nodes and weights for quadrature rules. User
%      inputs maximum number of points required, and the type required.
%      The default type is Gauss--Lobatto (QCase = 2), as it is of
%      higher order than Newton--Cotes.
%
%      David De Wit    July 13 1992 - July 17 1992

%%%%%%%%%%%%%%%%%%%%%%%%%%%%%%%%%%%%%%%%%%%%%%%%%%%%%%%%%%%%%%%%%%%%%%%%

if ~exist('R'),      R = 20;      end
if ~exist('QCase'), QCase = 2; end

%%%%%%%%%%%%%%%%%%%%%%%%%%%%%%%%%%%%%%%%%%%%%%%%%%%%%%%%%%%%%%%%%%%%%%%%

if (QCase == 1)
    if (R > 10)
        R = 10;
        sprintf('R too large for Newton--Cotes. Now R = 10.\n');
    end
    QRw = [
        1  1  1  7  19  41  751  989  2857  16067;
        1  4  3  32  75  216  3577  5888  15741  106300;
        0  1  3  12  50  27  1323  -928  1080  -48525;
        0  0  1  32  50  272  2989  10496  19344  272400;
        0  0  0  7  75  27  2989  -4540  5778  -260550;
        0  0  0  0  19  216  1323  10496  5778  427368;
        0  0  0  0  0  41  3577  -928  19344  -260550;
        0  0  0  0  0  0  751  5888  1080  272400;
        0  0  0  0  0  0  0  989  15741  -48525;
        0  0  0  0  0  0  0  0  2857  106300;
        0  0  0  0  0  0  0  0  0  16067
    ]
    QRw = QRw(1:R+1,1:R);          QRt = zeros(QRw);
    for j = 1:R
        QRw(1:j+1,j) = QRw(1:j+1,j)/sum(QRw(:,j));
        QRt(1:j+1,j) = [0:j]'/j;
    end
elseif (QCase == 2)
    QRt = zeros(R+1,R);          QRw = QRt;
    for j = 2:R+1
        [QRt(1:j,j-1), QRw(1:j,j-1)] = lobatto(j,0,1);
    end
end
end

```

A.7 hpmeth.m

```

function [lEip] = hpmeth(DMax, GMax, p, sigma, QCase);

% function [lEip] = hpmeth(DMax, GMax, p, sigma, QCase);
%
%       Experiment with h-p integration methods.
%
%       David De Wit   July 9 1992 - July 17 1992

%%%%%%%%%%%%%%%%%%%%%%%%%%%%%%%%%%%%%%%%%%%%%%%%%%%%%%%%%%%%%%%%%%%%%%%%

if ~exist('QCase'), QCase = 2;   end
if ~exist('sigma'), sigma = 0.15; end
if ~exist('p'),      p = 6;      end
if ~exist('GMax'),  GMax = 6;    end
if ~exist('DMax'),  DMax = 19;   end

%%%%%%%%%%%%%%%%%%%%%%%%%%%%%%%%%%%%%%%%%%%%%%%%%%%%%%%%%%%%%%%%%%%%%%%%

% Geometrically-graded h-p method.

Ehp = zeros(DMax,1);           vN = Ehp;
for D = 1:DMax
    G = [0 sigma^(D:-1:0)]';    S = [2:D+2]';
    [t, w] = hprmesh(G, S, QCase, 0);
    Ehp(D) = funchp(t)*w;      vNhp(D) = length(t);
end
lvNhp = log10(vNhp);          lEhp = log10(Ehp);

%%%%%%%%%%%%%%%%%%%%%%%%%%%%%%%%%%%%%%%%%%%%%%%%%%%%%%%%%%%%%%%%%%%%%%%%

% Various linear h and p methods. Variable g, constant p.

Eip = zeros(DMax,GMax);
for D = 1:DMax
    N = 2*D;
    for g = 1:GMax
        G = ([0:N]'/N).^g;
        [t, w] = hprmesh(G, p, QCase, 0);
        vN(D) = length(t);      Eip(D,g) = funchp(t)*w;
    end
end

lvN = log10(vN);              lEip = log10(Eip);

sprintf('Order %f, slopes of the blue lines are approximately', p)
(lEip(DMax-1,:) - lEip(DMax,:))./(lvN(DMax-1)-lvN(DMax))

plot(lvNhp,lEhp,'+r',lvNhp,lEhp,'-g',lvN,lEip,'+r',lvN,lEip,'-b');
xlabel('log10(points)');      ylabel('log10(error)');
text(0.9,0.7,'g = 1','sc');   text(0.9,0.57,'g = 2','sc');
text(0.9,0.45,'g = 3','sc');  text(0.9,0.35,'g = 4','sc');
text(0.9,0.27,'g = 5','sc');  text(0.9,0.2,'g = 6','sc');
text(0.7,0.15,'h-p method','sc'); grid;

%%%%%%%%%%%%%%%%%%%%%%%%%%%%%%%%%%%%%%%%%%%%%%%%%%%%%%%%%%%%%%%%%%%%%%%%

```

```

% Compare h methods for quadrature rules of various p (# points).

OMax = 12;
for p = 2:2:OMax
    g = p;
    for D = 1:OMax
        N = 2*D;
        [t, w] = hprmesh(G, j, QCase, 0);
        Ehhp(D,j-1) = funchp(t)*w;
    end
end

lhhN = log10(hhN);
lEhhp = log10(Ehhp);

sprintf('Slopes of the blue lines are approximately')
(lEhhp(DMax-1,:) - lEhhp(DMax,:))./(lhhN(DMax-1)-lhhN(DMax))

plot(lvNhp,lEhp,'+r',lvNhp,lEhp,'-g',lhhN,lEhhp,'+r',lhhN,lEhhp,'-b');
xlabel('log10(points)');
ylabel('log10(error)');
text(0.9,0.76,'p = 1','sc');
text(0.9,0.5,'p = 5','sc');
text(0.9,0.32,'p = 9','sc');
text(0.7,0.15,'h-p method','sc');
text(0.9,0.62,'p = 3','sc');
text(0.9,0.4,'p = 7','sc');
text(0.85,0.2,'p = 11','sc');
grid;

```

A.8 hprmesh.m

```

function [t, w] = hprmesh(G, S, IClosed)

% function [t, w] = hprmesh(G, S, IClosed)
%
%       Create a new quadrature rule, based on a mesh G, where between
%       points G(i) and G(i+1) is a (closed) quadrature rule of
%       Gauss--Lobatto type on S(i) points, including the 2 end points
%       G(i) and G(i+1); for i = 1:length(G)-1. If IClosed is 1, then
%       the contour is closed, and the ends are tied together. This
%       function is a generalisation of rmesh.
%
%       David De Wit   July 13 1992 - December 2 1992

%%%%%%%%%%%%%%%%%%%%%%%%%%%%%%%%%%%%%%%%%%%%%%%%%%%%%%%%%%%%%%%%%%%%%%%%

if ~exist('G'),          sigma = 0.1; G = [0 sigma.^(3:-1:1) 1]'; end
if ~exist('S'),          S = [2:5]';          end
if ~exist('IClosed'), IClosed = 1;          end

lG = length(G);          lS = length(S);
if ((lG ~= lS+1) & (lS ~= 1))
    sprintf('hprmesh: Danger l(G) = %f, l(S) = %f', lG, lS)
end

% Set up S for rules with a constant integration rule.
if (lS == 1), S = ones(lG-1,1)*S; end

dG = diff(G);            S = S - 1;
N = max(S);              R = length(dG);

% Obtain the nodes and weights in a table
QRt = zeros(N+1,N);      QRw = QRt;
for j = 2:N+1
    [QRt(1:j,j-1), QRw(1:j,j-1)] = lobatto(j,0,1);
end

% Play with the table
QRw(N+1,:) = diag(QRw(2:N+1,1:N))';          QRt(N+1,:) = ones(1,N);
for i = 2:N, for j = 1:i-1, QRt(i,j) = NaN; QRw(i,j) = NaN; end, end
tt = QRt(:,S);                                tw = QRw(:,S);
j = ones(N+1,1);                               tw = tw.*(j*dG');
tt = tt.*(j*dG') + j*G(1:R)';
tw(1,2:R) = tw(1,2:R) + tw(N+1,1:R-1);
tw1 = tw(1:N,:);                               tt1 = tt(1:N,:);
t = [tt1(:); tt(N+1,R)];                       t(isnan(t)) = [];
w = [tw1(:); tw(N+1,R)];                       w(isnan(w)) = [];

if (IClosed == 1)
    N = length(t);
    w = [w(2:N-1); w(1)+w(N)];                 t = t(2:N);
end

```

A.9 lobatto.m

```
function [x, w] = lobatto(n, a, b)

% function [x, w] = lobatto(n, a, b)
%
%      Return the weights w and points x of the n-point Gauss--Lobatto
%      quadrature rule on the interval [a, b].
%      See G. H. Golub, SIAM Review 1973 p 318.
%
%      Graeme Chandler          July 1992

%%%%%%%%%%%%%%%%%%%%%%%%%%%%%%%%%%%%%%%%%%%%%%%%%%%%%%%%%%%%%%%%%%%%%%%%

n = round(n);

if (n == 2)
    x = [a; b];
    w = [1; 1]*(b-a)/2;
elseif (n == 3)
    x = [a; a+(b-a)/2; b];
    w = [1; 4; 1]*(b-a)/6;
elseif (n >= 4)
    nn = n-1;
    m = 1:2:2*nn-1;
    m = (1:nn-1) ./ sqrt(m(1:nn-1) .* m(2:nn));
    J = (diag(m,-1)+diag(m,1));
    I = eye(nn);
    en = (1:nn)' == nn;
    gam = (J + I)\en;
    mu = (J - I)\en;
    sol = [1 -gam(nn); 1 -mu(nn)]\[-1; 1];
    alpha = sol(1);
    beta = sqrt(sol(2));
    [ww,xx] = eig([J beta*en; beta*en' alpha]);
    [xx, i] = sort(diag(xx));
    w = ww(1,i).^2 * (b-a);
    x = [a; (a+b)/2+(b-a)*xx(2:nn)/2; b];
end
```

A.10 rmesh.m

```
function [t, w] = rmesh(G, t1, w1, IClosed);

% function [t, w] = rmesh(G, t1, w1, IClosed);
%
% Create a new quadrature rule, based on a mesh G, where a
% (closed) quadrature rule (t1, w1) is inserted over each
% interval of G. If IClosed is 1, then the contour is closed,
% and the ends are tied together. This function is generalised
% into hprmesh. Originally conceived by Graeme Chandler.
%
% David De Wit July 13 1992 - September 6 1992
%
%%%%%%%%%%%%%%%%%%%%%%%%%%%%%%%%%%%%%%%%%%%%%%%%%%%%%%%%%%%%%%%%%%%%%%%%

if (length(G) < 2), return; end

if (length(G) ~= 2)
    h = diff(G);
    n = length(h);
    tw(1,2:n) = tw(1,2:n) + tw(m,1:n-1);
    w = [tw1(:); tw(m,n)];
    tt = t1(1:m-1)*h' + ones(m-1,1)*G(1:n)';
    t = [tt(:); G(n+1)];
    tw = w1*h';
    m = length(w1);
    tw1 = tw(1:m-1,:);
else
    t = t1;
    w = w1;
end

if (IClosed == 1)
    N = length(t);
    w = [w(2:N-1); w(1)+w(N)];
    t = t(2:N);
end
```

A.11 testcb.m

```

function N = testcb(C, sigma, Dmin, Dmax, Omin, Omax, alpha)

% function N = testcb(C, sigma, Dmin, Dmax, Omin, Omax, alpha)
%
%       Run cbiem for various parameters, and tabulate results.
%
%       David De Wit   May 12 1992 - December 21 1992

%%%%%%%%%%%%%%%%%%%%%%%%%%%%%%%%%%%%%%%%%%%%%%%%%%%%%%%%%%%%%%%%%%%%%%%%

if ~exist('alpha'), alpha = 1/2; end
if ~exist('Omax'), Omax = 16; end
if ~exist('Omin'), Omin = 8; end
if ~exist('Dmax'), Dmax = 19; end
if ~exist('Dmin'), Dmin = 16; end
if ~exist('sigma'), sigma = 0.32; end
if ~exist('C'), C = 7; end
format short e;                                format compact

%%%%%%%%%%%%%%%%%%%%%%%%%%%%%%%%%%%%%%%%%%%%%%%%%%%%%%%%%%%%%%%%%%%%%%%%

for D = Dmin:Dmax
    for O = Omin:2:Omax
        P = cbiem(C, D, sigma, O, alpha);
        if ((P ~= Inf) & (P ~= NaN))
            N(D-Dmin+1, (O-Omin)/2+1) = P;
        else
            N(D-Dmin+1:Dmax-Dmin+1,:) = ...
                Inf*ones(Dmax-D+1,(Omax-O)/2 + 1);
            return
        end
    end
    if (min(N(D-Dmin+1,:)) > 1)
        N(D-Dmin+2:Dmax-Dmin+1,:) = ...
            Inf*ones(Dmax-D,(Omax-Omin)/2+1);
        return
    end
end
end

```

References

- [1] Ivo Babuška and Milo R. Dorr. Error estimates for the combined h and p versions of the finite element method. *Numerische Mathematik*, 37:257–277, 1981.
- [2] George Francis Carrier, Max Krook, and Carl E. Pearson. *Functions of a Complex Variable: Theory and Technique*. McGraw-Hill, New York, 1966.
- [3] Graeme A. Chandler. Quadrature methods for boundary integral equations. In *Proceedings of the Mini-Conference on the Numerical Solution of Integral Equations*, Canberra, 1990. To appear.
- [4] Graeme A. Chandler. Discrete norms for the convergence of boundary element methods. In Gerd Dziuk, Gerhard Huisken, and John Hutchinson, editors, *Proceedings of the Centre for Mathematics and its Applications (Workshop on Theoretical and Numerical Aspects of Geometric Variational Problems)*, volume 26, pages 62–78, Canberra, 1991.
- [5] Graeme A. Chandler and Ivan G. Graham. Product integration-collocation methods for noncompact integral operator equations. *Mathematics of Computation*, 50(181):125–138, January 1988.
- [6] Philip J. Davis and Philip Rabinowitz. *Methods of Numerical Integration*. Academic Press, Orlando, 2nd edition, 1984.
- [7] Thomas K. DeLillo and Alan R. Elcratt. A comparison of some numerical conformal mapping methods for exterior regions. *SIAM Journal on Scientific and Statistical Computing*, 12(2):399–422, March 1991.
- [8] J. W. Dold. An efficient surface-integral algorithm applied to unsteady gravity waves. *Journal of Computational Physics*, 103:90–115, 1992.
- [9] Lawrence K. Forbes. A numerical method for non-linear flow about a submerged hydrofoil. *Journal of Engineering Mathematics*, 19:329–339, 1985.
- [10] Eugene C. Gartland, Jr. Graded-mesh difference schemes for singularly perturbed two-point boundary value problems. *Mathematics of Computation*, 51(184):631–657, October 1988.
- [11] Gene Howard Golub. Modified matrix eigenvalue problems. *Siam Review*, 15(2):318–334, April 1973.
- [12] W. Gui and Ivo Babuška. The h , p and h - p versions of the finite element method in 1 dimension. Part I: The error analysis of the p version. *Numerische Mathematik*, 49:577–612, 1986.
- [13] W. Gui and Ivo Babuška. The h , p and h - p versions of the finite element method in 1 dimension. Part II: The error analysis of the h and h - p versions. *Numerische Mathematik*, 49:613–657, 1986.
- [14] W. Gui and Ivo Babuška. The h , p and h - p versions of the finite element method in 1 dimension. Part III: The adaptive h - p version. *Numerische Mathematik*, 49:659–683, 1986.

- [15] Theodore V. Hromadka II. *The Complex Variable Boundary Element Method*, volume 9 of *Lecture Notes in Engineering*. Springer-Verlag, Berlin, Heidelberg, New York, Tokyo, 1984.
- [16] Theodore V. Hromadka II and G. L. Guymon. A complex variable boundary element method: Development. *International Journal for Numerical Methods in Engineering*, 20(1):25–37, January 1984.
- [17] Theodore V. Hromadka II and G. L. Guymon. Reducing relative error from the CVBEM by proper treatment of the known boundary conditions. *International Journal for Numerical Methods in Engineering*, 20(11):2113–2120, 1984.
- [18] A. J. Kassab and C. K. Hsieh. Application of the complex variable boundary element method to solving potential problems in doubly connected domains. *International Journal for Numerical Methods in Engineering*, 29(1):161–179, 1990.
- [19] F. V. Postell and Ernst P. Stephan. On the h , p and h - p versions of the boundary element method – numerical results. *Computer Methods in Applied Mechanics and Engineering*, 83:69–89, 1990.
- [20] Siegfried Prößdorf and A. Rathsfeld. Quadrature and collocation methods for singular integral equations on curves with corners. *Zeitschrift für Analysis und ihre Anwendungen*, 8(3):197–220, 1989.
- [21] W. W. Schultz and S. W. Hong. Solution of potential problems using an overdetermined complex boundary integral method. *Journal of Computational Physics*, 84(2):414–440, 1989.
- [22] Ernst P. Stephan. The h - p version of the Galerkin boundary element method for integral equations on polygons and open arcs. In Carlos Alberto Brebbia, editor, *Conference of Boundary Element Methods – 10*, Southampton, England, 1988.
- [23] Gilbert Strang and George J. Fix. *An Analysis of the Finite Element Method*. Automatic Computation. Prentice-Hall, Englewood Cliffs, New Jersey, 1973.